

REVIEW ARTICLE

Three-dimensional bioprinting of artificial blood vessel: Process, bioinks, and challenges

Ya-Chen Hou^{1,2,3}, Xiaolin Cui⁴, Zhen Qin^{1,2,3}, Chang Su^{1,2,3}, Ge Zhang^{1,2,3}, Jun-Nan Tang^{1,2,3*}, Jing-An Li^{5*}, Jin-Ying Zhang^{1,2,3*}

¹Department of Cardiology, The First Affiliated Hospital of Zhengzhou University, Zhengzhou, Henan, China

²Henan Province Key Laboratory of Cardiac Injury and Repair, Zhengzhou, Henan, China

³Henan Province Clinical Research Center for Cardiovascular Diseases, Zhengzhou, Henan, China

⁴School of Medicine, The Chinese University of Hong Kong, Shenzhen, China

⁵School of Material Science and Engineering and Henan Key Laboratory of Advanced Magnesium Alloy and Key Laboratory of Materials Processing and Mold Technology (Ministry of Education), Zhengzhou University, 100 Science Road, Zhengzhou, China

(This article belongs to the *Special Issue: Fine-tuned Hydrogels for 3D Bioprinting*)

Abstract

The coronary artery bypass grafting is a main treatment for restoring the blood supply to the ischemic site by bypassing the narrow part, thereby improving the heart function of the patients. Autologous blood vessels are preferred in coronary artery bypass grafting, but their availability is often limited by due to the underlying disease. Thus, tissue-engineered vascular grafts that are devoid of thrombosis and have mechanical properties comparable to those of natural vessels are urgently required for clinical applications. Most of the commercially available artificial implants are made from polymers, which are prone to thrombosis and restenosis. The biomimetic artificial blood vessel containing vascular tissue cells is the most ideal implant material. Due to its precision control ability, three-dimensional (3D) bioprinting is a promising method to prepare biomimetic system. In the 3D bioprinting process, the bioink is at the core state for building the topological structure and keeping the cell viable. Therefore, in this review, the basic properties and viable materials of the bioink are discussed, and the research of natural polymers in bioink, including decellularized extracellular matrix, hyaluronic acid, and collagen, is emphasized. Besides, the advantages of alginate and Pluronic F127, which are the mainstream sacrificial material during the preparation of artificial vascular graft, are also reviewed. Finally, an overview of the applications in the field of artificial blood vessel is also presented.

Keywords: Three-dimensional bioprinting; Tissue-engineered vascular grafts; Artificial blood vessel; Bioink; Decellularized extracellular matrix

*Corresponding authors:

Jun-Nan Tang
(fcctangjn@zzu.edu.cn)
Jing-An Li
(lijingan@zzu.edu.cn)
Jin-Ying Zhang
(jyzhang@zzu.edu.cn)

Citation: Hou Y-C, Cui X, Qin Z, et al., 2023, Three-dimensional bioprinting of artificial blood vessel: Process, bioinks, and challenges. *Int J Bioprint*, 9(4): 740. <https://doi.org/10.18063/ijb.740>

Received: July 31, 2022

Accepted: October 02, 2022

Published Online: April 28, 2023

Copyright: © 2023 Author(s). This is an Open Access article distributed under the terms of the Creative Commons Attribution License, permitting distribution, and reproduction in any medium, provided the original work is properly cited.

Publisher's Note: Whioce Publishing remains neutral with regard to jurisdictional claims in published maps and institutional affiliations.

1. Introduction

Cardiovascular disease is the leading cause of morbidity and mortality worldwide, with an estimated 17.8 million deaths/year (233.1/100,000)^[1]. Bypass surgery is a conventional

treatment for cardiovascular disease, through which blood grafts are used to bypass the blockage, and about 450,000 patients undergo bypass surgery in the United States alone in a year^[2]. Organ transplantation is one of the most important research topics in the 21st century. Despite the improved quality of transplantation and the increased survival rate in recent decades, organ shortage is still the biggest challenge remaining to be overcome. Tissue engineering was proposed by Joseph P. Vacanti in 1980 who put forward some theoretical basis about artificial organs.

The human vascular system is a complex network of blood vessels of various sizes, and the blood vessel is constituted by vascular endothelial cells (EC, which form the intima), vascular smooth muscle cells (SMC, which form the tunica), and fibroblasts^[3-5]. The extracellular matrix (ECM) is used as the supporting structure and filling material^[6]. At present, commercially available artificial implants are made from polymers called expanded ePTFE (Gore-Tex) or PET (Dacron), both of which can be prepared into various large-diameter (>6 mm) blood vessels for storage^[7,8]. However, the polymer vessels are hard, rough, and highly hydrophobic, resulting in poor biocompatibility and activation of the blood coagulation cascade; therefore, the polymer is not suitable for small-diameter artificial vessels^[9,10].

From the perspective of bionics, three-dimensional (3D) printing is the most ideal method to obtain artificial blood vessels with different functions by forming the three cells according to their distribution in natural blood^[11,12]. The conventional 3D bioprinting is based on the additive manufacturing, which adopts layer-by-layer stacking of special print and bioink to combine organ cells^[13]. The core issue of 3D printing is to choose the suitable and functional bioink to load the cells at designated locations^[14]. The bioinks should have better biocompatibility, structural stability, and enough mechanical and rheological properties, especially the ability to allow cell adhesion, proliferation, and diffusion^[15]. The hydrogels contain a large number of water and porous microstructures, which provide the nutrient substances to cells^[16]. Besides, due to their mechanical properties and the ability to change their physical state between liquid and solid using simple methods, hydrogels are regarded an important bioink for 3D printing. The prime candidate hydrogels can be divided into synthetic polymers and natural polymers^[17]. The synthetic polymers mainly contain Pluronic F-127 and polyethylene glycol (PEG), while the natural polymers comprise alginate, fibrous protein, hyaluronic acid (HA), and collagen^[18]. Nevertheless, the hydrogel is too weak to undergo surgical procedures and high pulse pressure of the blood pressure. To improve the properties, a suitable method for cross-linking hydrogel has to be chosen. The principal cross-linking methods can be divided into two

categories: (i) Adding chemical cross-linking agents or using various chemical reactions to form irreversible covalent bonding between polymer chains and (ii) using physical cross-linking by H bond and electrostatic attraction, which results in hydrogels with weaker mechanical properties but better biocompatibility^[19-21].

Although no clinical cases of bioprinting of vessels or vascular structures have been reported, progress in this regard has been noted in several animal experiments. For example, artificial blood vessels prepared by poly(L-lactide-co-caprolactone)-heparin/silk gel were implanted into the carotid artery of New Zealand white rabbits in 2020. It was found that the lumen could form a continuous endodermis 8 months after surgery^[22]. **Figure 1** shows the papers in the field over the past 20 years^[23] and the patent application status in the past 10 years with data derived from the database of the Patent Office. In this review, the necessary properties of artificial blood vessels, the cross-link method, and the type of hydrogel were discussed to evaluate the possible candidate materials in 3D bioprinting area of the artificial blood vessel.

2. Performance requirement of hydrogel

2.1. Physical performance requirements

The ultimate aim of the artificial blood vessel is to mimic the structure and function of human blood vessels. Based on the “Cardiovascular implants and extracorporeal systems – vascular grafts and vascular patches – *in vitro* systems tubular vascular grafts and vascular patches (ISO 7198: 2016),” simulating the mechanical properties of the human internal mammary artery is the main purpose of artificial blood vessel^[24]. The theoretical and actual burst strength of the natural blood vessel are 3775 and 3099 mmHg, respectively^[25]. The systolic blood pressure of hypertensive patient can reach 180 mmHg, so the artificial blood vessel made with the polymer should have a rupture pressure of 1000 mmHg with natural tissue compliance of 10–20%/100 mmHg and tensile strength of >1 MPa^[26]. The properties of the hydrogel and the artificial blood vessels are discussed in this subsection to present the basic standard for guiding the perpetration process^[27]. Besides, the tensile strength of the natural blood vessel ranges from 0.2 – 0.6 MPa to 2 – 6 MPa. It is important for the artificial vessels to have similar mechanical properties^[28]. The artificial blood vessel with a diameter of 18–24 mm can be used for the replacement of artificial blood vessel in the thoracic aorta, and the artificial blood vessel with a diameter of 6–10 mm can be used for the diversion of artificial blood vessel in the arteries of extremities and neck. The main mechanical properties of the natural blood vessel and artificial blood vessel are listed in **Table 1**.

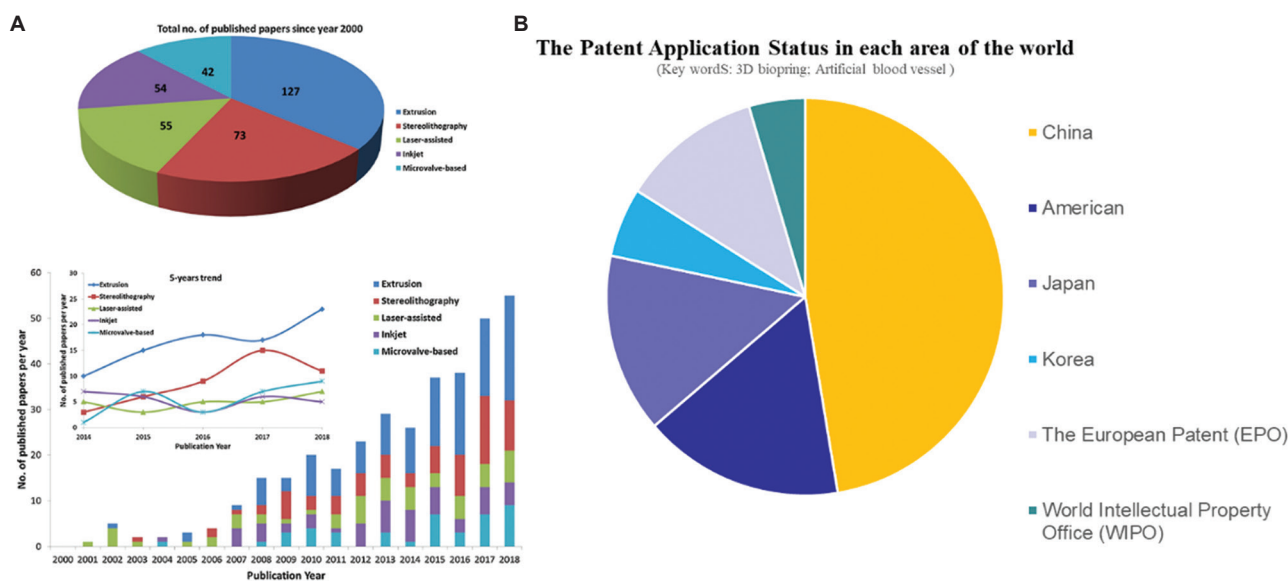


Figure 1. (A) Papers in the field over the past 20 years^[23], and (B) the patent application status in the past 10 years with data derived from the database of the Patent Office. Figure 1A reproduced from ref.^[23] with permission from Elsevier B.V. (License Number: 5398071195762).

Table 1. Mechanical properties of natural blood vessel and artificial blood vessel

Mechanical properties	Natural blood vessel	Artificial blood vessel
Burst pressure	3775 mmHg	1000 mmHg
Tensile strength	0.2–0.6 MPa to 2–6 MPa	>1 MPa
Diameter	18–24 mm (thoracic endovascular aortic repair); 6–10 mm (other blood vessel)	
Suture retention	Yes	Yes
Kink and compression resistance	Yes	Yes
Maintenance of a functional endothelium	Yes	Yes
Low manufacturing costs		Yes
Easy storage		Yes

2.2. Hydrogel requirements

The main properties of the hydrogel or bioink include shear thinning, yield stress, viscosity, and molding ability that may be influenced by the embedded cell^[29]. Shear thinning is a phenomenon in which the viscosity decreases with the increase of shear stress, and it is caused by the untangling and orientation of polymer chain during the flow of polymer solution^[30]. Especially for extrusion type bioink, non-Newtonian fluid behavior occurs during extrusion, which increases the shear rate and reduces the viscosity^[31]. During the printing process, bioink must shift from high-viscosity gel to low-viscosity fluid, and then, the internal structure is quickly renewed, thereby improving the viscosity to maintain the structural integrity^[32]. Thus, the basic of shear thinning is proper viscosity behavior, which is usually described in terms of storage (or elastic) modulus G' and loss (or viscous) modulus G'' ^[33]. The loss modulus G'' measures the energy dissipated by a

material and is related to viscous flow^[34]. An increase in the viscosity of hydrogel slows down the flow and deformation, thereby reducing the possibility of collapse of the topological structure during the primary and secondary cross-linking^[35]. However, higher viscosity could result in plugging around the injection port. Changing the molecular weight and concentration of polymer, or adding modifier, are some of the approaches used to enhance the viscosity. For example, the viscosity of 1.5% HA is about 22 Pa·s, the viscosity of collagen at a concentration of 1.5 – 1.75% is around 1.7 – 1.8 Pa·s^[36]. Taken together, the influence of viscosity on the performance of bioink should be considered comprehensively^[37].

In addition to meet the basic rheological properties and mechanical properties, the cellular compatibility of the hydrogels also needs to balance during preparation^[38]. The bioink is the only environment that supports and provides nutrition to the cells; on the contrary, the existence of the

cells influences the physical properties and forming ability of hydrogels^[39]. Before printing, the hydrogels need to keep the cell in suspended state; during extrusion printing, the cell activity will be influenced significantly by the stress. After the forming process, the solid printed structure needs to ensure the smooth transport of nutrients^[40]. The inserted cells will occupy specific positions in the bioink, which may affect the cross-linking efficiency and viscoelasticity of the bioink^[41]. In the HA hydrogel, the gelation time remains the same with a cell density of 2.5×10^7 cell/mL; however, the gelation time increases from 20 to almost 60 min when the cell density rises to 1×10^8 cell/mL. After the cell density achieving $2.50 - 5.0 \times 10^8$ cell/mL, the HA cannot cross-link as usual, resulting in a significant decrease in viscosity^[42]. Billiet *et al.* found that the blending of cells impacts solution viscosity. Above the gelation temperature, the viscosity decreased by 2-fold until the cell density reached 1.5×10^6 cell/mL. Increasing the cell density further to 2.5×10^6 cell/mL increased this factor to 4^[43]. Cell metabolism also affects the chemical process of cross-linking; for instance, the reactive oxygen species produced by photoinitiators can be absorbed by cells, decreasing the efficiency of cross-linking^[44].

2.3. Forming requirements

The blood vessel is a structure that delivers blood under hemodynamic pressure; thus, the artificial blood vessels must be strong enough to withstand the pressures^[45]. Burst pressure compliance, anti-fatigue perfusion, *in vivo* graft effectiveness, and suture retention are the most important criteria for vascular graft selection^[46]. Bursting pressure is the maximum pressure; the graft can withstand before the occurrence of acute leakage. This pertains to the relation between the maximum circular force (σ) and burst pressure (P) per unit area. From the formula $\sigma = Pd/2t$, the bursting pressure increases as the diameter decreases, which means that the burst pressure of the small-caliber blood vessel will be higher than that of the normal caliber blood vessel^[47]. Therefore, the microvessel structure prepared using hydrogel has higher requirement on strength^[48].

Besides, the stiffness (elasticity) of vascular structure is an important attribute that determines cell activity. Several studies found that the cell migration decreased with an increase of stiffness, and the differentiation of marrow mesenchymal stem cells (MSCs) is also dependent on hydrogel stiffness^[49,50]. Compared with MSCs cultured on 100 kPa hydrogels, the MSCs cultured on 30 kPa hydrogels secrete more immunomodulatory and regenerative factors, indicating that the MSC differentiation may be determined by the stiffness of basement: The soft, medium hardness, and hard basements could facilitate the differentiation of the MSCs into nerve cells, muscle cells, and bone-like

cells, respectively^[51-53]. The proliferation rate of EC varies with the hardness of their growth surface, and all the experimental results pointed to the importance of stiffness as a determinant of cellular behavior^[53].

At present, the mechanism of the printing process with hydrogels or bioinks loaded with cells for a long term is not very clear^[54]. The shear forces always contribute to the deformation of cells, leading to the rearrangement of the cytoskeleton after a few rounds of printing process^[55]. The change of cellular morphology has been found to regulate the cell behavior and differentiation^[56]. For example, the MSCs differentiate into osteogenic lineages on the stimulation of stretch^[57], and the stretching state induces the EC to release more nitric oxide^[58]. Thus, the external and internal factors that influence the cell behavior are complex and related to many physical factors, as shown in Figure 2. Therefore, a deep understanding of the factors underlying cell stress would help lay a foundation in the relevant bioprinting protocol in the future^[59-61].

3. Bioinks for 3D bioprinting

With the rapid development of material printing, many companies have developed bioinks for specific tissue engineering applications; for example, Organovo's Novo-Gel has been used for bioprinting aortic vascular grafts^[62]. It is difficult for the existing hydrogel system to fulfill the requirements, such as attaining the same mechanical property of some organs and the optimal biocompatibility^[63]. The novel bioink should always be strategically designed based on the requirements of the arterial blood vessel and prepared using suitable cross-linking methods and composite recipe. According to the function of hydrogel in the printing process, the hydrogels are classified into support materials and scarified materials, and the support materials are further categorized into natural and synthetic polymers^[64]. The major reason that the bioprinting of arterial blood vessel would fail is the lack of intact inner intima, which leads to platelet adhesion and aggregation as well as thrombosis^[65,66]. It is better to use the EC as the bioprinting materials to rebuild the inner intima as soon as possible. The shear force from the nozzle could influence the micromorphology and function of the bioprinted cells, decreasing the adhesion, proliferation, and viability of cells^[67]. Thus, the other purpose of the hydrogels is to protect the cells during the printing process^[68]. In this section, the advantages of each hydrogel in the preparation of arterial blood vessel are discussed.

3.1. Support hydrogel

3.1.1. Synthesis hydrogel

As proven by the U.S. Food and Drug Administration (FDA), PEG is a biocompatible material, whose main chain

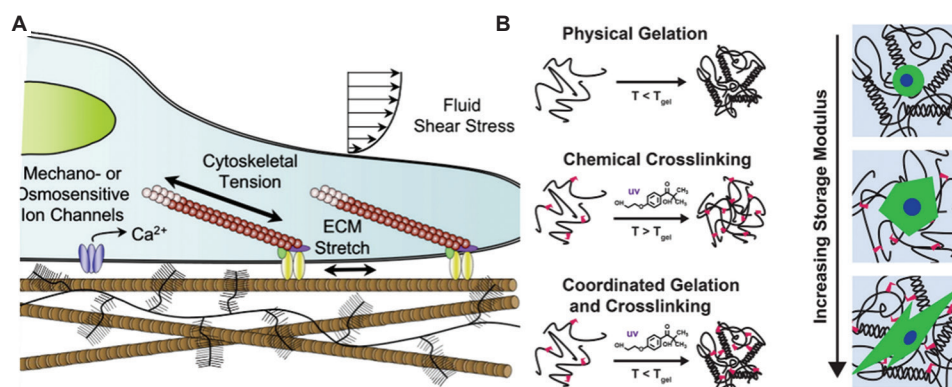


Figure 2. (A) Transduction of mechanical factors and the regulation of stem cell fate^[60]. (B) The difference of physical and chemical gelation below the thermal gel point and the morphological change of cell with the stiffness of the hydrogel^[61]. Figure 2B reproduced from ref. ^[61] with permission from John Wiley and Sons, Inc. (License Number: 5355060311460).

is (-CH₂-CH₂-O-), indicating that the material is bioinert and not suitable to be directly used as a bioink^[69]. The use of dimethacrylate and diacrylate modified PEG (named as PEGDMA) is possible to improve its performance as bioink^[70]. The PEGDMA could increase the EC adhesion and proliferation after adding GelMA to form complex hydrogel^[71]. To further improve the properties of the PEG, 4-arm poly (ethylene glycol)-tetra-acrylate (PEGTA) has been synthesized. The presence of multiple active cross-linking sites on the PEGTA could increase the strength and keep the porous structure after cross-linking^[72]. Compared with PEGDMA, PEGTA with porous structure could promote cell growth and diffusion within the gel and increase the rapid exchange of nutrients. PEGTA, which has a low molecular weight (3350 g/mol), could be cleared by the kidneys to ensure biosafety^[73]. More importantly, adding 3 – 4% w/v nanosilicates (nSi) into the poly(ethylene glycol)-dithiothreitol could obtain better shear-thinning characteristics and precision deposition ability during the printing process, as shown in Figure 3^[74].

3.1.2. Natural hydrogel

(A) HA

HA, which is a major component of ECM, is a linear and non-sulfated glycosaminoglycan consisting of alternating units of β-1, 4-D-glucuronic acid, and β-1, 3-n-acetyl-d^[75]. HA has good flexibility, biocompatibility, biodegradation, and bio-absorbability, and its high porosity is conducive to the exchange of nutrients^[76]. With the rich negative charges in its structure, HA can absorb a great deal of water and then increase its volume by 1000 times, forming a loose hydration network that acts as a sieve to control water transport and limit the movement of pathogenic plasma proteins and protease into the matrix network, thus playing a key role as an immune modulator and anti-inflammatory factor^[77]. HA also shows antioxidant effects for its ability to react with oxygen-

derived free radicals^[78]. Pure HA is not suitable for direct use as bioink because HA aqueous solutions give viscous shear-thinning preparations a neat prevalence of viscous modulus, implying that no yield stress and no shape retention will be resulted on printing. Thus, HA is always combined with other hydrogel for use as bioink^[79]. There are two methods to use HA as a bioink: (i) Using HA in the form of a single or multiple chemical derivatives as the main constituent and (ii) using HA with natural polymer to enhance the mechanical property of the structure^[80]. A HA-g-pHEA-gelatin is created by cross-link polymerization of hydroxyethyl acrylate (HEA) to HA and then grafting of gelatin-methacryloyl by radical polymerization. With 6 and 8% concentrations of methacrylic anhydride, the hydrogel showed excellent printability and cellular biocompatibility^[81]. Small-diameter (4.0 mm) and heterogeneous double vascular structure were made with GelMA, HA, glycerin, and gelatin, together with EC and SMC that construct the inner and outer tissue so as to mimic natural blood vessels and maintain high cell viability and proliferation^[82].

The normal cell seeding process is divided into two steps: (i) Printing the 3D hollow structure using a variety of hydrogels and using the sacrificial material to create the hollow and (ii) seeding the cells on the inner wall^[83]. Although this strategy is widely used to manufacture the arterial blood vessel, another strategy, which relies on the enzymatically digestible photopolymers, has also been used in the same process^[84]. HA could be hydrolyzed into smaller molecules by hyaluronidase; the special properties are involved in the printing process to control degradation kinetics, which introduce further changes to the geometry of the implants, rather than dissolving the material completely. The application of hyaluronidase enables the creation of hollow structures of any geometry^[85]. By applying this knowledge, Thomas *et al.* printed vessel mold with EC, which demonstrated better cellular viability (28 days).

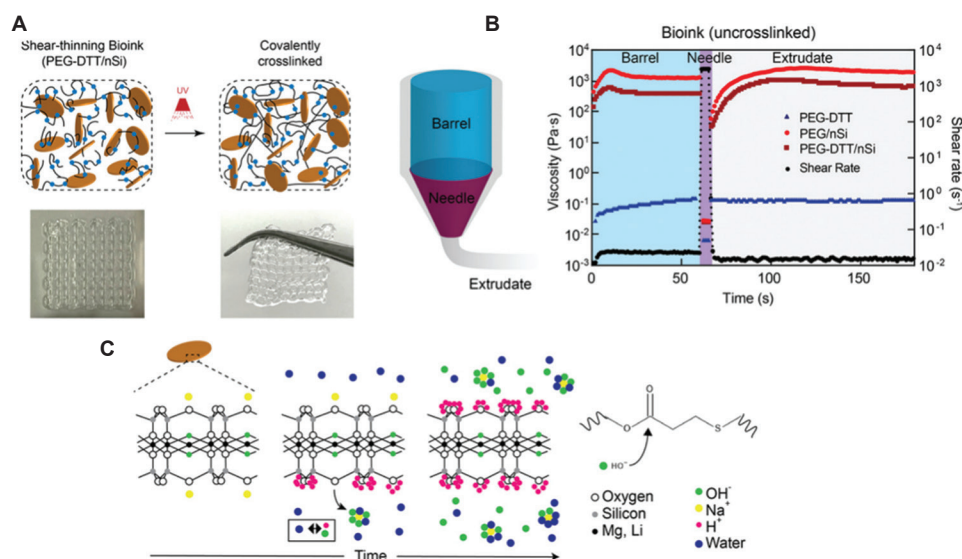


Figure 3. (A) Schematic showing interaction of poly(ethylene glycol)-dithiothreitol (PEGDTT) and nanosilicates before and after cross-linking. The inset shows printability of PEGDTT/nSi bioink. (B) Schematic of printing process through barrel, needle, and on printing bed. (C) Proposed mechanism of nanoparticle-induced degradation of PEGDTT^[74]. Figure 3 reproduced from ref. ^[74] with permission from John Wiley and Sons, Inc. (License Number: 5355130231370).

HA is a kind of low cross-linked hydrogel solution that exhibits non-Newtonian behavior. Cross-linking by chemical, enzymatic, physical, or photo-cross-linking mechanisms could enhance the mechanical property of the HA blood vessel. The most common sites for HA chemical modification are the carboxyl ($-\text{COOH}$) and primary (C6) hydroxyl ($-\text{OH}$) groups on D-glucuronic acids^[86]. Two HA derivative-based bioinks have been reported, namely, HA methacrylate (HAMA) and tyramine-modified HA (HA-Tyr)^[87]. HAMA could confer the photo-cross-linking ability to HA, and ultraviolet (UV) cross-linking could enhance the long-term structural stability and provide better shape fidelity^[88,89]. About 3% w/v HAMA could be used as single composition to print tissue containing MSCs. HAMA with 12 kinds of complementary hydrogels supplemented with 5% gelatin has been studied systematically to find a suitable complex bioink system. The results in Figure 4A show that the 0.5 wt% HAMA could not support the structure, and adding 2.5 wt% GelMA confers better properties to the printed bone tissue^[90]. The HA-Tyr has better cellular biocompatibility as it could cross-link under the green light^[91]. After mixed with the nanocellulose, the shear-thinning characteristics and mechanical stability of HA were increased and the cells were bestowed the ability to differentiate^[92]. As shown in Figure 4B, Li *et al.* used the HAMA synthesized with low-molecular-weight HA and alginate to produce microvessels, which have better mechanical strength and enable the free migration of EC with outstanding angiogenesis function^[93].

To enhance the differentiation of MSC after bioprinting, a biofunctional peptide having an SH-group in the N-terminal has been connected on the acrylated HA through Michael addition in a two-step reaction^[94]. This hydrogel had higher viscosity and better mechanical integrity after the cells were embedded in it^[95]. Besides, the traditional 3D bioprinting blood vessel relies on the sacrificial materials and the layers of support materials. A novel method, which is based on a self-healing hydrogel made of HA, is suitable for the bioprinting arterial blood vessel due to its high precision and supramolecular self-assembly characteristics^[96]. Adamantane (Ad) or β -cyclodextrin (β -Cd) was used to modify HA to form Ad-HA and Cd-HA, which can then rapidly form supramolecular assemblies by intermolecular guest – primary bonds^[97]. After filling other bioinks using syringe needle, this kind of hydrogel will change the shape, and then, the Ad-HA and CD-HA will fix itself to support the constructor of the bioinks. For example, the MSCs could be printed to format the shape of the vessel and then the fibroblast 3T3 cell population could be used to print the first MSC constructor^[98]. To improve the mechanical property and storage modulus of this system, Irgacure 2959 was added to the system for second photo-cross-linking, as shown in Figure 5^[99,100].

(B) Collagen

Collagen is one of the key proteins in ECM and is also a core biological material for the application of 3D bioprinting of artificial blood vessels^[101]. Collagen has two $\alpha 1(\text{I})$ chains

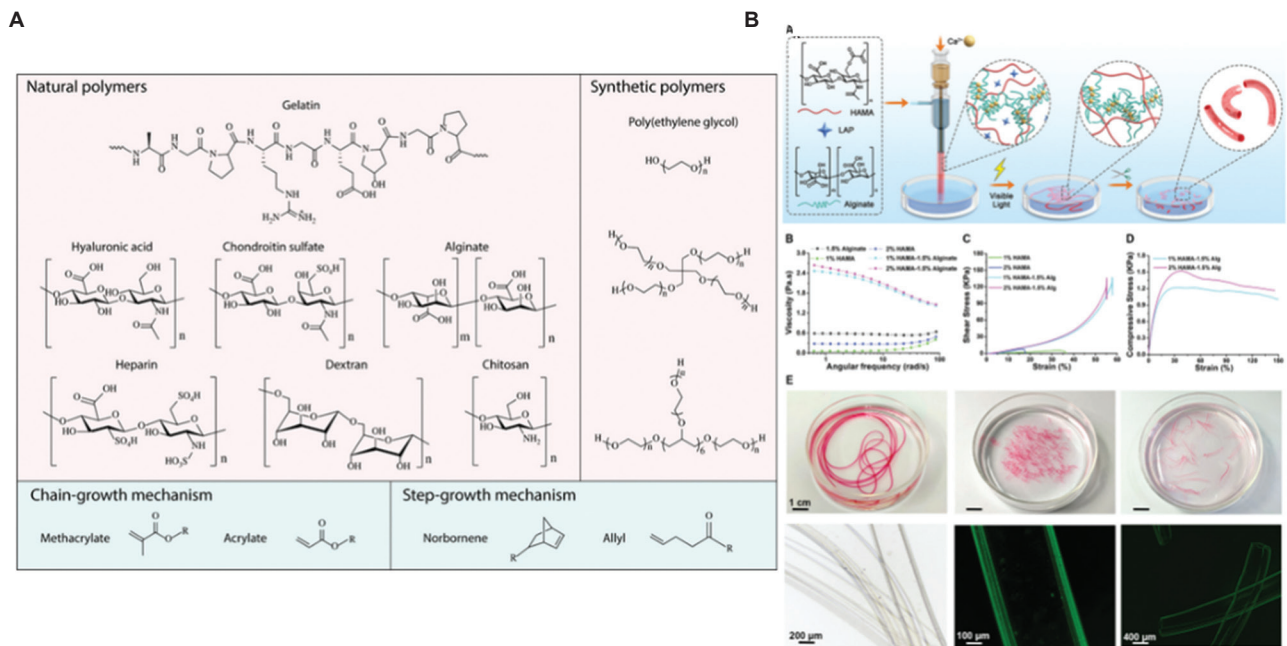


Figure 4. (A) Polymer backbones and photo-cross-linkable side groups used in the study reported in^[90]. Dithiothreitol was used as cross-linker in the step-growth mechanism. (B) Schematic depiction of the preparation of customizable HAMA/alginate-based microtubes^[93]. Figure 4B reproduced from ref. ^[93] with permission from John Wiley and Sons, Inc. (License Number: 5355220749244).

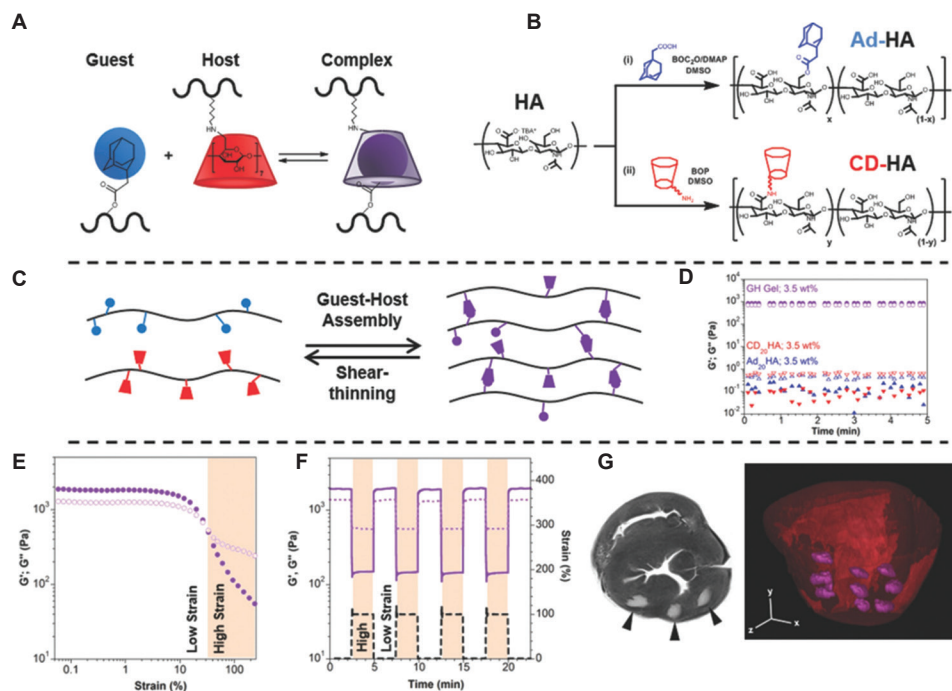


Figure 5. Guest-host hydrogel formation enables shear-thinning injection and hydrogel retention^[99]. Figure 5 reproduced from ref. ^[99] with permission from John Wiley and Sons, Inc. (License Number: 5355231470261).

and one $\alpha 2(I)$ chain, and the repetitive nature of the amino acid sequence consists of $-[\text{Gly}(\text{glycine})-\text{X}-\text{Y}]_n-$, where X and Y are always proline and hydroxyproline residues^[102].

Collagen bioinks show excellent biocompatibility and can self-assemble to form hydrogels under physiological conditions^[103]. The cross-linking time of collagen is

longer than 1 h at room temperature, which decreases the structural fidelity and mechanical strength. Thus, enhancing the storage modulus of the ink is the principal direction of improving the collagen bioinks. One of the methods is to increase the collagen concentration in solution. Some studies showed that single-component collagen with a concentration of higher than 20 mg/mL could be used to create accurate 3D structures, and it is important to note that the cell encapsulation and activity could always be influenced by higher concentrations. Therefore, using the methacrylate group to modify the collagen allows the photopolymerization of the hydrogel without causing protein denaturation, and this kind of hydrogel is known as methacrylated collagen (ColMA) or carboxymethyl agarose. ColMA contains small randomly oriented fibers, which allow spontaneous fibrous self-assembly and keep cell activity as normal collagen with enzymatic biodegradability. ColMA still contains small randomly oriented fibers, which could spontaneous fibrous self-assembly and keep cell activity as normal collagen with enzymatic biodegradability^[104]. Another frequently used method is adding cross-linking agent: For example, the collagen cross-linked by 1-ethyl-3-(3-dimethylaminopropyl)-carbodiimide and N-hydroxysuccinimide had the strength of 853 kPa and 1000 kPa, respectively^[105,106]. Muthusamy *et al.* added the xanthan gum into the collagen to form the collagen-XG as bioink, and the hydrogel could support the EC to form a network of interconnected blood vessels^[107].

(C) Gelatin

Gelatin is a denatured form of collagen, with high viscosity, good biocompatibility, and degradation ability *in vivo*. However, gelatin is a thermal gel that turns into a solution above 37°C, and the printing accuracy is so low that it cannot be directly used as bioink^[108]. Therefore, combining gelatin with other biological materials or chemical modification is the main method of applying gelatin^[109]. GelMA is a photo-cross-linked hydrogel formed by modified gelatin with methacryloyl group (MA), and the chemical modification of gelatin only involves less than 5% of the amino acid residues in molar ratio, which will not significantly decrease the arginyl-glycyl-aspartic acid (RGD) content of the gelatin^[110]. The RGD, which is a fragment of GelMA, gives EC better adhesion and differentiation abilities^[111]. The matrix metalloproteinases on the GelMA enable the marking and degradation of the complex by enzyme^[112]. Due to the existing lots of primary amine (-NH₂) and hydroxy (-OH), which are unsaturated photo-cross-linkable groups, the GelMA is easy to polymerize under the light-induced condition. Besides, GelMA could be cured by reduction-oxidation reaction, heating, gamma irradiation or electron beam,

and other methods. Meanwhile, photoinitiators such as lithium phenyl (2,4,6-trimethylbenzoyl) phosphinate (LAP) and Irgacure 2959 are more suitable for bioprinting the arterial blood vessel^[113]. The advantages of Irgacure 2959, which is the most common photoinitiator, include being slightly soluble in water and having low cytotoxicity without UV irradiation^[114]. After irradiation, Irgacure 2959 can efficiently generate free radicals and cross-link the required content, culminating with an acceptable level of cell survival^[115]. Nevertheless, the UV (337 nm) may induce endogenous oxidative damage to deoxyribonucleic acid (DNA) through the action of reactive oxygen species^[116].

The cross-linking method of HAMA and GelMA is similar, and using the mixture of the two hydrogels could create adjustable 3D microenvironment to regulate cell behavior^[117]. Due to the very low viscosity, the pure HAMA is difficult to maintain the shape of the printed object. Adding 6% – 12% GelMA into 4% HAMA could increase the print resolution and regulate the tissue stiffness. The mixture could also support the encapsulated cells and regulate the cellular response^[118]. In theory, the ideal ink should exhibit gelatinous properties (the storage modulus G' is dominant and higher than 200 Pa) and shear-thinning behavior for high-fidelity printing. To further reinforce the bioink made by HAMA-GelMA, the cellulose nanocrystals (CNCs) were added into the system. The structure printed by HAMA-GelMA-CNCs could keep the printed structure stable after 20% strain circulation^[119]. Besides, the fidelity of printed filaments could be improved by mixing HAMA with GelMA. Mouser *et al.* found that the yield stress of GelMA/gellan/HAMA was relatively high and the addition of HAMA increased the stability of the filament^[120]. The filaments made of 10% GelMA began to collapse after bridging an 8 mm gap, but following the addition of HAMA, a single filament can close a gap of 16 mm^[120]. Nguyen *et al.* studied the cytotoxicity under 405 nm light and found that the concentration below 17 mmol/L (0.5 wt%) did not induce obvious cytotoxicity^[121]. Yin *et al.* used LAP as the photoinitiator to prepare the GelMA/gelatin bioink^[122], as shown in Figure 6. The shear-thinning behavior and the biocompatibility of the 5% GelMA and 30% gelatin were higher than those of the pure 5% GelMA, and the swelling behavior of the GelMA/gelatin was lower than that of the 5% GelMA^[122].

The proportion of methacryloyl substituents in GelMA is another factor that influences cross-linking density and modulus of compressibility^[123]. After light curing the low concentration (5 wt%) GelMA with 0.5 wt% Irgacure 2959 at 5 mW/cm² for 300 s, the cells had better embedded cell properties. On the other hand, it is very difficult to culture cells with high concentration GelMA. Therefore, the mechanical properties of GelMA-based 3D-bioprinted

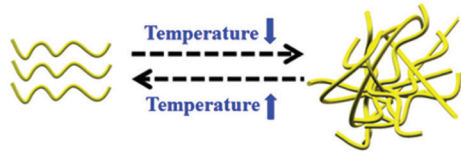
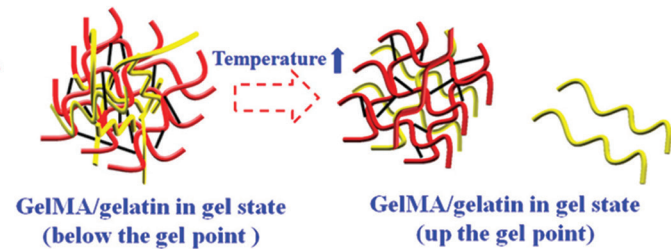
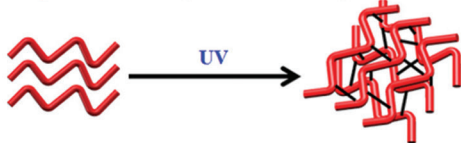
Step 1: Reversible thermo-crosslinking of gelatin**Step 2: Irreversible photo-crosslinking of GelMA**

Figure 6. Two-step cross-linking of GelMA/gelatin bioinks^[122]. **Figure 6** reprinted (adapted) with permission from “Yin J, Yan M, Wang Y, *et al.*, 2018, 3D Bioprinting of Low Concentration Cell-Laden Gelatin Methacrylate (GelMA) Bioinks with a Two-Step Cross-linking Strategy. *ACS Appl Mater Interfaces*, 10(8): 6849–57.” Copyright 2018 American Chemical Society.

structures and the cellular viability of these structures are related to the degree and concentration of GelMA methacrylate^[124]. Jin *et al.* loaded SMC in the GelMA bioink and printed the outer layer of a tubular structure and then seeded the EC on the surface of the internal surface to form a bionic vascular vessel with dual layers^[125]. After 7 days of culture, the SMC distributed in the outer layer showed long spindle shape, and the cell survival rates were $95.62 \pm 1.31\%$. The CCK-8 absorption value of EC was 0.315 ± 0.0179 , indicating that the structure has better proliferation ability^[125].

GelMA/catechin groups can rapidly cross-link to form artificial vessels with core-shell structure with human coronary artery smooth muscle cells, and EC is encapsulated in the shell and inner layer. This kind of vessel had better bionic properties and could connect with normal blood vessel in 2 weeks and finish the rebuilding of the structure in 6 weeks^[126]. Cui *et al.* designed a GelMA/polyethylene (ethylene glycol) diacrylate/alginate hybrid gel containing lyase and SMC. The complex had better ability to exchange the nutrient substance and improve the cell proliferation^[127]. With the alginate being gradually degraded by lyase, more space is made available with the alginate is gradually degraded by lyase, more space had been^[127]. Ruther *et al.* also used the double-needle extrusion systems to prepare a 4 mm vessel with fibroblast (normal human dermal fibroblasts) and EC on the outer and inner sides of the structure, and the vessel could improve the cell vitality and migration in 3 weeks^[128].

GelMA-based bioinks showed good biocompatibility with cells due to the presence of RGD peptide. Nevertheless, the challenges of using GelMA as bioink remain, especially in extrusion printing. Zhuang *et al.* have proposed a layer-

by-layer UV-assisted bioprinting strategy to fabricate complex 3D bioprinting structures with high aspect ratios using GelMA-gellan gum bioink for tissue engineering of soft tissues^[129]. To strike a balance between printability and biocompatibility, a minimum yet ideal amount of gellan gum was added to enhance the printability of the bioink without compromising biocompatibility^[129].

3.1.3. Decellularized extracellular matrix (dECM)

The ECM of vascular tissues is special in both composition and topology, and the dynamics and reciprocity between the cells and the microenvironment are fundamental to the stable existence of blood vessel^[130]. However, these features cannot be completely simulated by single materials, and the embedded cells are not able to rebuild the cell-cell connections and microenvironments of 3D cell tissues^[131]. Li *et al.* discovered ECM at MeHA, a biocompatible bioink with suitable mechanical support and visible printable properties, which contains thermosensitive ECM, methacrylate hyaluronic acid, and photoinitiator (Eosin Y, TEOA, and NVP)^[132]. As shown in **Figure 7**, the bioprinting strategy based on extrusion and digital light processing successfully encapsulate cells, and the cell viability rate was maintained at $94.27 \pm 3.00\%$ after 7 days^[132]. Pati *et al.* developed a new dECM from the porcine dermal tissue, which had better mechanical and biocompatibility^[133]. The cross-linking conditions were detected by Pati *et al.*^[132] The results showed that the 3% dECM is a suitable concentration for 3D printing system. The pH of the extracted acidic dECM needs to be regulated to physiological condition, and it has to be kept below 10°C before cell embedding. This dECM is a kind of heat-sensitive material, which could be in solution state below 15°C and turn into a gel after the temperature rises to 37°C. This bioink was extruded

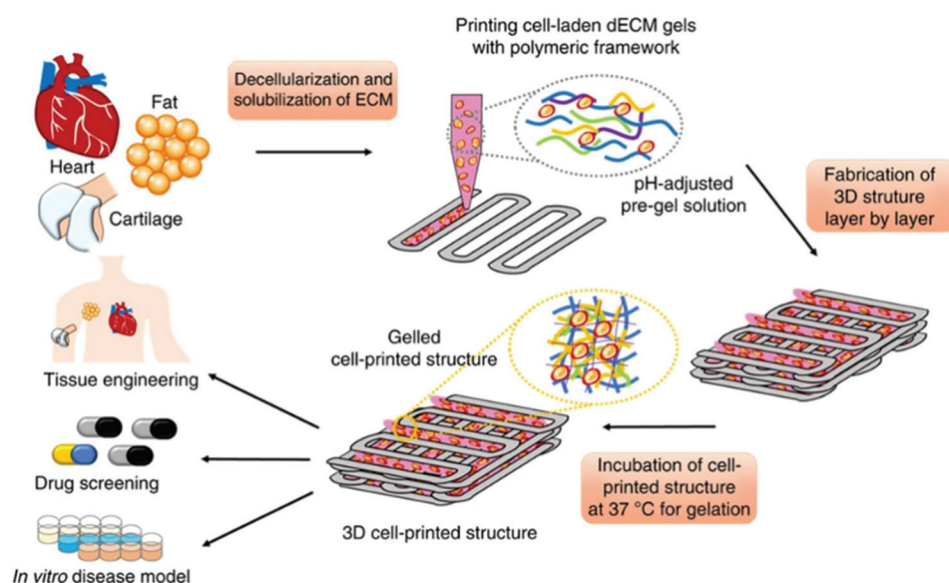


Figure 7. Schematic diagram of the preparation of 3D-bioprinted scaffolds loaded with cells using visible light cross-linking^[134].

in filamentous form and 1–10 layers of structure were successfully printed. The bioink could protect the cell in the extrusion process, and the structure can be potentially used in cardiac remodeling^[131,134].

In addition to the dECM, the Matrigel is also important in the 3D bioink system. In 1988, Bilozur *et al.* found that Matrigel could increase the proliferation of neural crest cells^[135]. Matrigel is the first ECMs synthesized with laminin in the developing embryo at two-cell stage, which has a profound effect on the cell differentiation^[136]. Therefore, the Matrigel has been used to culture various kinds of undifferentiated embryonic stem cells^[137]. It is hard to simulate the connection and signal transduction pathway using artificial materials, especially in rebuilding blood vessel^[138]. There has been a surge of relevant studies in the past decade pointing out a clear path to improve the resemblance of fabricated tissue to natural tissue^[139]. The microenvironment composed by the ECM plays an important part in guiding and mediating stem cell differentiation and proliferation, and some researchers found that the cell-ECM interactions are extremely complex in nature^[140].

3.1.4. DNA material

The advantages of the DNA hydrogel include its mechanical strength and non-expansion/contraction characteristics with outstanding ability to keep the cells alive^[141]. DNA is a nucleic acid composed of a nitrogen base and a phosphate skeleton. According to the Watson-Crick base pairing principle, DNA is a highly programmable material that can achieve high-precision self-assembly at the molecular level

and confer excellent biocompatibility to the material^[142]. In 1996, Nagahara *et al.* reported the first polymeric hydrogel containing DNA^[143]. Following the pioneering work, many DNA hydrogels had been studied^[144].

Wu *et al.* chose human serum albumin, a naturally abundant plasma protein, to construct the polypeptide backbone of the hydrogel, added PEG to increase water content, and reduce non-specific protein absorption; the synthesis of a protein-DNA hybrid hydrogel is shown in Figure 8A^[142,145]. Li *et al.* studied a supramolecular polypeptide-DNA hydrogel, which was first used in the 3D bioprinting system, as shown in Figure 8B and C. The polypeptide-DNA hydrogel was combined with two kinds of bioinks, namely, Bioink A and Bioink B. Bioink A is a polypeptide-DNA conjugate, while Bioink B is a double-stranded DNA, which consists of two “sticky ends” with sequences complementary to the sequences on the single-stranded DNA on Bioink A. Both Bioink A and Bioink B could format the hydrogel under phosphate-buffered saline in seconds and the G’ is about 5000 Pa, indicating that the hydrogel is capable of self-supporting after printing^[146]. The hydrogel has dual-enzymatic responsiveness: The polypeptide backbone could be degraded by the endoproteinase, and the nuclease would cut the DNA linkers in 24 h. In further study, after adding the cells into the DNA-hydrogel, it was found that the ink could help the cell suspended in solution and keep the cells active for a long time, and the cell survival rate could reach 98.81% at the initial stage of printing^[147]. Hydrogels uses cross-linking between polypeptide-DNA and DNA linker and guides protein synthesis *in situ*. The basic theory that relies on this is the

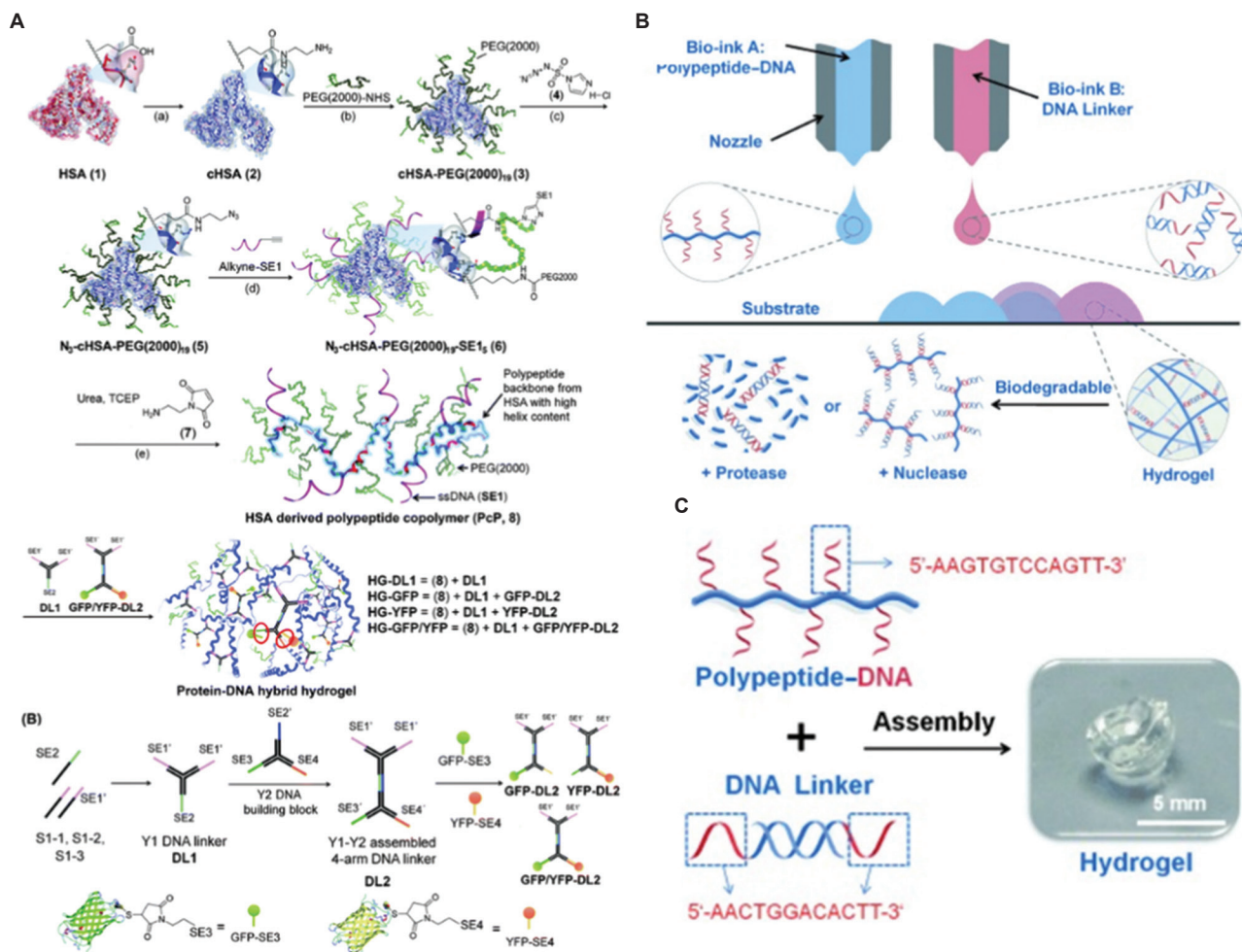


Figure 8. (A) Synthesis of a protein-DNA hybrid hydrogel^[146]. (B) 3D bioprinting of the polypeptide-DNA hydrogel to fabricate arbitrarily designed 3D structures. (C) Preparation of the polypeptide-DNA hydrogel using the two components^[147]. **Figure 8A** reproduced from ref.^[146] with permission from Royal Society of Chemistry (Order Number: 1250780). **Figure 8B and 8C** reproduced from ref.^[147] with permission from John Wiley and Sons, Inc. (License Number: 5355800472548).

central dogma of molecular biology: DNA acts as a template to make mRNA (messenger RNA), which is translated into proteins that regulate cell behavior^[148]. Park *et al.* used a cell-free system to prepare the protein using DNA gels^[149]. The cell-free protein-producing hydrogel (a “P-gel”) could produce 16 proteins at very minute level (in mg/mL), and compared with traditional method, the P-gel could be used as bioink in artificial tissue^[149]. The polypeptide-DNA hydrogel is a promising cross-linking strategy after bioprinting that could fabricate items with better mechanical property and could produce special protein to regulate the cell’s behavior. Thus, this bioink is promising in terms of biocompatibility, tissue maturation, and functional regeneration.

3.1.5. Other hydrogels

The fibrin, agarose, and nanocrystalline cellulose play an important part in the areas of bioprinting and bioink. The

fibrous protein, which has a randomly arranged fibrous network, participates in the clotting process^[150]. Fibrous protein also supports the EC proliferation in the bioink by directing associated cells to growth factors, such as vascular endothelial growth factor and fibroblast growth factor, to promote angiogenesis, and shows shear rigidity under high strain to mimic the non-linear elastic behavior of soft tissue^[150-152]. Therefore, the fibrous protein can be combined with other hydrogels to enhance the mechanical property and tissue remodeling. Freeman *et al.* added the fibrous protein into the gelatin to bioprint the blood vessel structure with rupture pressure reach 1110 mmHg, which is about 52% of that in human’s great saphenous vein^[153]. Li *et al.* used the Pluronic F-127 (10% w/v) as scarified rod materials and printed fibrous protein/gelatin on it to form the blood vessel structure, with a burst pressure of only about 1000 mmHg, which is lower than the minimum

standard^[154]. To enhance mechanical property, the sodium alginate and carbon nanotubes were mixed in the fibrous protein/gelatin^[154].

Agarose is a natural polysaccharide with a hot gel temperature of 30 – 40°C^[155]. Agarose has good mechanical properties since it is inert, it is difficult for cells to attach and proliferate on its surface^[156]. The 5% agarose-alginate mixture is more suitable to be used as extruded bioink without the additional cross-linking steps or as scarified material to ensure high structural fidelity^[157]. Combining carboxymethyl-hexanoyl chitosan (CA) hydrogels (8% w/v) with Pluronic F-127 could build the vessel structure under the parametric design, which creates vessel structure by expressing parameters in an algorithm^[155,158].

Nanocellulose refers to three types of nanomaterials: Bacterial nanocellulose (BNC), cellulose nanofilaments, and CNCs^[159]. Among them, BNC can be synthesized by bacteria, such as *gluconacetobacter xylinus*, in glucose and xylose medium and secreted in the form of extracellular polysaccharide to produce structural hydrogels with a length of about 100 µm and a diameter of about 100 nm^[160].

3.2 Scarified hydrogels

3.2.1. Pluronic F-127

Pluronic F-127 is a kind of synthesized block copolymers that combine with hydrophilic polyethylene oxide and two hydrophobic polypropylene oxides on both sides^[161]. Below 10°C, Pluronic F-127 is at liquid state but it could self-assemble at room temperature, and the structure could be dissolved in 4°C cold water to form hollow structure^[162]. Pluronic F-127 is bioinert to many cells, easy to print, and stress free to cells during formation. These features make Pluronic F-127 a promising support and scarified hydrogel^[160,163]. Xu *et al.* used Pluronic F-127 as a sacrificial material to form the blood vessel through a multi-nozzle 3D bioprinting system. After printing, Pluronic F-127 was removed to obtain multistage hollow channels for attaching EC, human aortic vascular smooth muscle cells, and neonatal dermal fibroblasts, as shown in [Figure 9A](#)^[166]. The structure and materials could provide better cellular biocompatibility and elastic modulus that are close to natural aorta^[164]. A biodegradable multilayered bioengineered vascular construct with a curved structure was prepared by Liu *et al.*^[165], as shown in [Figure 9B](#). The gelatin and Pluronic F-127 were used as vessel wall and scarified materials to build the vessel mold, while the inner channel of the structure was seeded with EC; this construct showed better cellular biocompatibility^[165]. O'Connell *et al.* used an on-board light exposure strategy that is capable of quick (<1 s) and direct cross-linking when the bioink is being extruded from the nozzle^[166].

On this basis, more stable and harder gels can be obtained by adding photo-cross-linking groups to the hydroxyl groups at the end of Pluronic F-127^[167]. For example, cross-linking acrylates to the hydroxyl group of Pluronic F-127 allows cross-linking under UV to produce a stable hydrogel and improve the printing properties, and the structure can sustain cellular activity for up to 14 days^[168]. Some studies have combined Pluronic F-127 with collagen and used Irgacure 2959 initiator to prepare bioink. The bioink shows shear-thinning behavior and has reversible sol-gel transformation related to temperature. It is relatively tough, elastic, and biocompatible with EC as well as can be prepared with an average diameter of 0.20 ± 0.01 mm and an average outer diameter of 0.74 ± 0.01 mm for the vessel structure^[169].

3.2.2. Alginate

The alginate is a kind of anion (negatively charged) hydrophilic polysaccharide derived from the brown seaweed^[170]. The properties are the same as those of GAG and could cross-link with many materials to form hydrogel^[171]. The disadvantages of the alginate hydrogel are the lack of porosity for nutrient substance exchange and the lack of adhesion properties, along with lower degradation rate *in vivo*, making it hard to be exclusively used in bioprinting^[172]. Normally, the alginate is cross-linked using the Ca²⁺ ions (calcium chloride or calcium sulfate solution) in ionic cross-linking, which means that the structure is reversible under the presence of ionic solution. The shell and core of the printing nozzle contain alginate bioink and calcium chloride solution, respectively, while calcium chloride solution can be used as a supporting structure for the direct printing of vessels structure^[173]. Thus, the alginate-Ca hydrogel system is a useful scarified complex to form the hollow structure of arterial blood vessel.

Gao *et al.* suspended the SMC and fibroblast in the alginate-Ca hydrogel and used two coaxial nozzles on the rotating rod to print artificial vessels to form SMC on the inner side and fibroblast on the outer side to simulate the structure of the vessel^[174], as shown in [Figure 10A](#). The ultimate strength of the structure is 0.184 MPa, and the survival rate of the cells embedded in the vessel exceeds 90% after being cultured for 7 days^[174]. Jia *et al.* also used the similar method to prepare the vascular constructs^[175]. The multilayer coaxial nozzle device was used to prepare highly organized perfusion vascular structures containing EC and MSC. This method could manufacture vessels of a wide range of diameters, with an average outer diameter of almost 500 – 1500 µm, an average inner about 400 – 1000 µm, and a wall thickness of around 60 – 280 µm, which allow perfusion, nutrient diffusion, and cell growth^[175]. Zhang *et al.* prepared arterial blood vessel with alginate-Ca

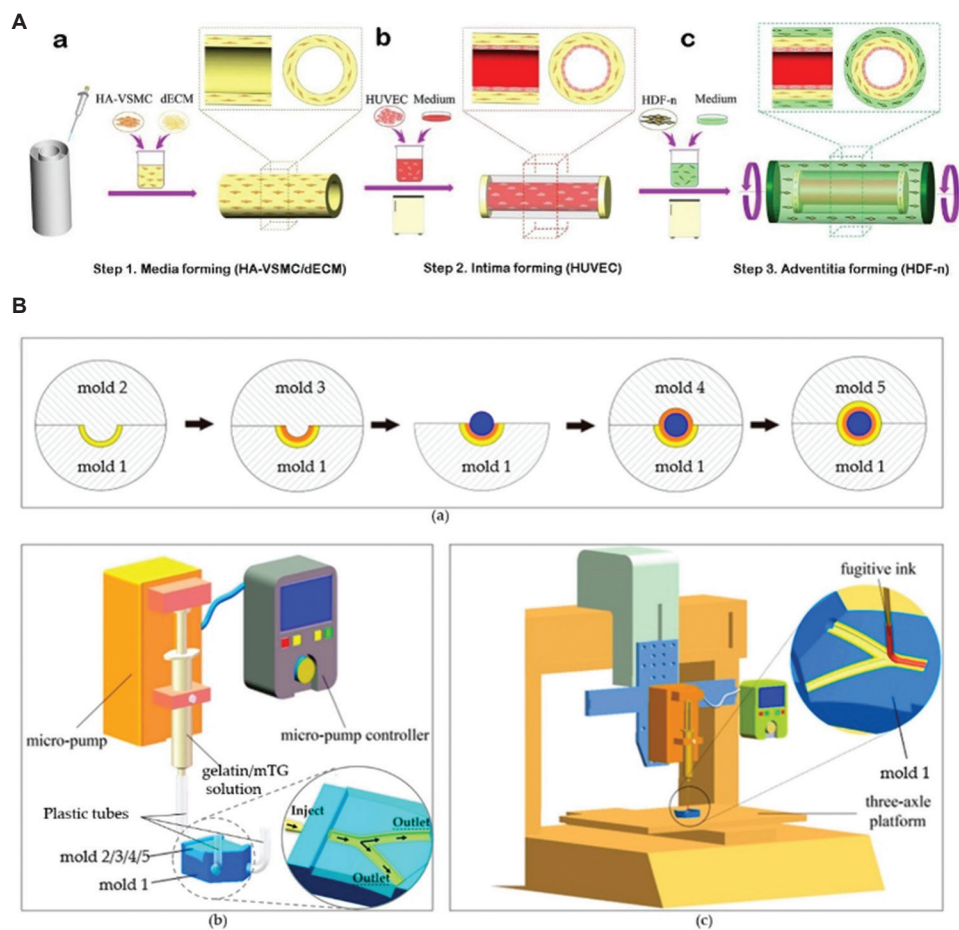


Figure 9. (A) Schematic diagram of the manufacturing process of the three-layer (3D) arteriovenous structure: intima media and adventitia^[66]. (B) A schematic representation of the step-by-step process of the fabrication of multilayered bifurcated tissue-engineered vascular grafts with a curved structure^[165].

hydrogel containing SMC by the sheath and core sections of the coaxial nozzle, with the vascular inner and outer diameters of $990 \pm 16 \mu\text{m}$ and $1449 \pm 27 \mu\text{m}$, respectively, and the human umbilical vein smooth muscle cells had better cell viability in the vessel hydrogel^[176]. Jang *et al.* used PCL, alginate, and EC to prepare a 4 mm arterial vessel, and the EC and alginate were contained within the PCL shells. The vessel implanted onto the bilateral carotid and femoral arteries in dogs had a patency rate of 64.3% after 2 weeks, and the embedded cells also had better viability^[177].

At present, cell-based 3D bioprinting is not suitable for commercial production due to several challenges, such as cell sedimentation membrane damage and cell dehydration. The traditional alginate hydrogels are ion cross-linked, indicating the poor stability and structure *in vivo*. Therefore, chemical modification of alginate to achieve secondary and covalent bonding is used to stabilize the performance. Karen *et al.* used 10 proline-rich peptide domains or seven repeats of a complementary

peptide to modify each alginate chain so as to obtain a new gel-phase bioink Mitch-Alginate^[178]. A weak hydrogel molecule was created between two complementary peptide domains to prevent cell sedimentation and provide mechanical protection from membrane damage, as shown in Figure 10B.

3.2.3. Discussion on the existing hydrogel

The main challenge of the artificial blood vessel is using suitable gels to prevent structural collapse, which is caused by the lack of the strength and stiffness^[179]. Table 2 shows the advantages and disadvantages of the bioink. Nevertheless, at present, bioinks with satisfactory mechanical, rheological, and biological properties have not yet been developed^[180]. Therefore, developing composite hydrogel offers a basic solution. Although the normal bioink could provide a “synthetic” environment to the cells, and the added factors could induce the cell behavior to some extent, it is still hard to simulate the real environment. Thus, the better solution

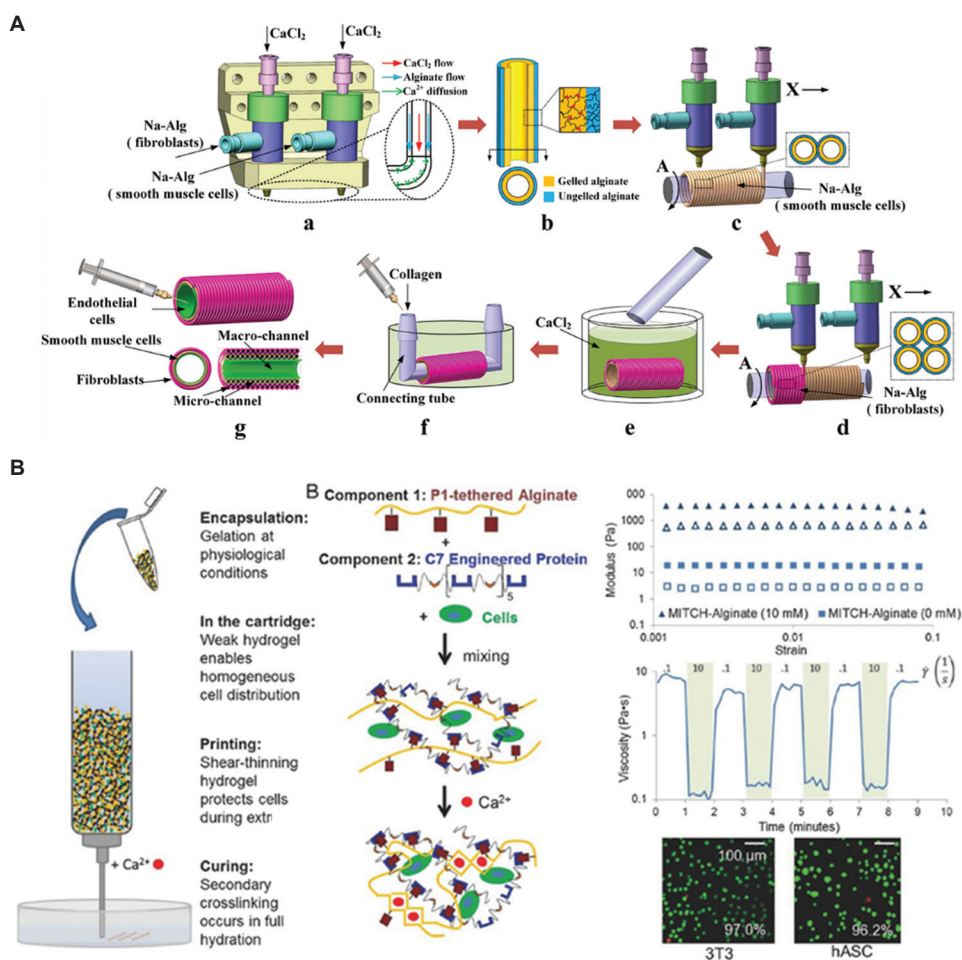


Figure 10. (A) Manufacturing process of 3D alginate container structures with multi-scale fluid channels^[174]. (B) Schematic depicting the benefits of Mitch-Alginate bioink for each stage of the printing process^[178]. **Figure 10A** reprinted (adapted) with permission from “Gao Q, Liu Z, Lin Z, *et al.*, 2017, 3D Bioprinting of Vessel-like Structures with Multilevel Fluidic Channels. *ACS Biomater Sci Eng*, 3(3): 399–408.” Copyright 2017 American Chemical Society. **Figure 10B** reproduced from ref.^[178] with permission from John Wiley & Sons, Inc. (License Number: 5355931318350).

is to use the natural ECM as the bioink to construct the organs to ensure higher cell viability and induce specific cell behavior. The natural ECM contains compounds and growth factors unique to natural tissues, but also with a topology that compounds cannot mimic. Nonetheless, it is difficult to produce the natural ECM required as purifying and extracting ECM is a time-consuming and labor-intensive procedure. Despite the ECM shortage, we believe that the ECM is the promising bioink which could fully simulate the complex environment of organs.

4. 3D bioprinting techniques

Bioprinting approaches include extrusion-based, inkjet-based, and stereolithography-based techniques. Among these approaches, extrusion-based bioprinting is the most common method due to fast fabrication speed, ease of operation, and compatibility with various bioinks. **Table 3**

demonstrates the advantages and disadvantages of different bioprinting techniques in blood vessel construction.

4.1. Material extrusion

Extrusion-based bioprinting platform is a promising method to form vascular structures^[181]. Norotte *et al.* discovered a method for scaffold-free fabrication of small-diameter blood vessels using spheroid or cylindrical-shaped aggregates containing SMCs and fibroblasts^[182]. The spheroid- or cylindrical-shaped aggregates were extruded by agarose rods and then fused to form single- or double-layered vessels with an outer diameter ranging from 0.9 to 2.5 mm^[182]. Park *et al.* demonstrated extrusion-based bioprinting of artificial blood vessel with a tubular structure by manufacturing a single strand of polyvinyl alcohol (PVA) as a core and printed a biocompatible polydimethylsiloxane (PDMS) filament coating. The PVA core could be removed by hydrogen

Table 2. Advantages and disadvantages of bioinks

Bioink	Advantages	Disadvantages
Hyaluronic acid/HAMA	Mimics the natural ECM	<ul style="list-style-type: none"> • High viscosity • Shear-thinning property • Photo-cross-linking • Easily modifiable to enhance cell regulatory activities
Collagen		<ul style="list-style-type: none"> • Highly hydrophilic • Not mechanically stable • Slow gelation rate
Gelatin/GelMA		<ul style="list-style-type: none"> • Biodegradability • ECM-mimic material in clinical application
dECM/Matrigel		<ul style="list-style-type: none"> • Good biological activity • Better printability • Shear-thinning behavior • Photo-cross-linking
DNA material	<ul style="list-style-type: none"> • Better mechanical strength • Shear-thinning behavior • Maintain cellular activity 	<ul style="list-style-type: none"> • Matrigel is obtained from murine sarcoma cells • Limited applicability for clinical translation (only Matrigel)
Agarose	<ul style="list-style-type: none"> • Better cell compatibility • pH response • Thermal gelling property 	<ul style="list-style-type: none"> • High cost
Nano-crystalline cellulose	<ul style="list-style-type: none"> • Shear-thinning behavior • Fast cross-linking • Relatively high stiffness 	<ul style="list-style-type: none"> • Lack of cell adhesion motifs • Non-degradable
Alginate	<ul style="list-style-type: none"> • As sacrificial structure • Better printability and rheological properties • Gels at room temperature • Dissolves when cooled 	<ul style="list-style-type: none"> • Lower shape fidelity if cells are added • Lower cell viability
Pluronic F-127		<ul style="list-style-type: none"> • Biological inert material • Slow degradation when not cross-linked • Low mechanical strength
		<ul style="list-style-type: none"> • Poor biocompatibility

HAMA: Hyaluronic acid methacrylate, dECM: Decellularized extracellular matrix, DNA: Deoxyribonucleic acid, ECM: Extracellular matrix

peroxide leaching under sonication, and the remaining PDMS tube was the artificial blood vessel^[183]. The extension technology of the extrusion bioprinting is a ferromagnetic soft catheter robot (FSCR) system. This magnetic actuation-based system controls bioprinting *in situ* with a computer a minimally invasive manner. The FSCR is designed by dispersing ferromagnetic particles in a fiber-reinforced polymer matrix, with stable bioink extrusion, and allows printing of a variety of materials with different rheological properties and biofunctionalities, and the superimposed magnetic field drives the FSCR to complete the printing process. This technology allows the minimally invasive biofabrication in a rat model^[179]. Even this method has not been used for *in situ* angiogenesis or rebuilding of the blood vessel system, it still improves the thought and field of vision.

Extruding-based bioprinting is a common and valuable method for fabricating artificial blood vessel. Although being popular due to its inexpensive and simple process, it has some limitations, such as low resolution and cell

damage due to shear stress during extrusion^[184]. Therefore, there is a trade-off between printability and cell viability in extrusion printing. On the one hand, the printed gel can be improved in terms of viscosity and yield stress of the gel, and higher pressure is needed when extruding with high extrusion shear stress, which could lead to cell damage. On the other hand, a smaller needle size is needed to improve the resolution, but smaller nozzle size yields higher pressure to guarantee continuous extrusion, which, however, leads to more serious cell damage. The bio ink is suitable for extrusion based bio printing that is cross-linked layer by layer under UV irradiation to increase structural stability, but it will also damage cell vitality. Therefore, changing the cross-link method and enhancing the ability of the gel to maintain cell activity are the main future directions.

4.2. Material jetting

The inkjet technique is capable of forming droplets in a volume range measured in picoliter and then launching

Table 3. The advantages and disadvantages of different bioprinting techniques in blood vessel construction

Bioprinting technique	Process	Cross-linking	Material	Cell	Resolution	System	Cost
Extrusion	Simple	<ul style="list-style-type: none"> • Light • Temperature • pH • Chemical 	<ul style="list-style-type: none"> • Viscous bioinks (30 mPa.s – 6×10^7 mPa.s) • Multi-material • Multi-material • Low viscous bioinks (3.5–12 mPa.s) 	<ul style="list-style-type: none"> • High densities • Moderate cell viability • Low cell density ($<10^6$ cells/mL) • High cell viability (80–90%) 	Low-to-medium	Low printing speed	Medium level
Jetting	Simple		<ul style="list-style-type: none"> • High variety of printable bioinks 	<ul style="list-style-type: none"> • Medium cell density (10^8 cells/mL) • High cell viability ($>85\%$) 	High (30 μ m)	Medium printing speed	Low
Stereolithography	Complex	Transparent and photosensitive bioink			High (~1 μ m)	Simultaneous cross-linking of the whole 2D layer avoids the need of X-Y movement	High

thousands of droplets in seconds through printing in a non-contact manner^[185]. The inkjet bioprinting methods are characterized by microdropletization as well as high-throughput, non-contact, and drop-on-demand process^[185]. The key factors of material jetting include biopaper, bioink, printing parameters, and 3D models. The biopaper, which is agar or collagen coating on the culture dishes to fix the cells and increase the cell viability, is especially important. However, the rigid substrate of the biopapers always influences the cell functions. Besides, the injection process exerts pressure to cells in bioink. Therefore, inkjet bioprinting has more restrictions on the viscosity of the bioink, which undoubtedly limits the choice of biomaterial for stimulus response. The bioink should have better biocompatibility, degradability, fluidity, and viscosity properties. The alginate and CaCl₂ have been widely used in inkjet bioprinting, and they are used in inkjet bioprinting methods to form alginate nanoparticles in CaCl₂ solutions and then assemble the particles into tubular structure^[186,187].

Being a non-contact printing method, inkjet printing is suitable for *in situ* bioprinting, where bioink is deposited directly onto injured tissue, and it has greater potential in clinical applications. 4D bioprinting is considered a mature version of 3D bioprinting for fabricating cell-laden structures. This method allows cells to adapt to the *in vivo* microenvironment from the very beginning, eliminating the need for *in vitro* culture. In the future, 4D-bioprinted objects could change their shape or physiological activity in response to physical or biological stimuli from the local microenvironment in the body, and fuse or act in concert with surrounding cells or tissues with better design. The picoliter level of high resolution enables the design of complex geometry, making inkjet printing the most likely method for single-cell printing, which allows cells to be arranged one by one without additional biomaterials to support or link them, thus accelerating the process of cell fusion^[188].

4.3. Vat polymerization

Vat polymerization is a 3D printing method that performs in a layer-by-layer manner using photopolymerization to fix the bioink in a vat into a construct^[189]. The flow properties of blood vessels are strongly dependent on their 3D shape. Therefore, it is essential to replicate the natural shape to accurately simulate *in vivo* flow conditions. The core technology of the vat polymerization takes into consideration the physiological requirements at macro- and micro-scales to optimize structure. To obtain accurate *in vivo* shape, computed tomography angiography scans of human organs are segmented into cross-section and converted to 3D model^[190]. Stereolithography, as

the primary technique of vat polymerization printing, enables relatively fast production of volumetric structures with precise internal and external architectures. Stereolithography was developed in the 1980s and was one of the first commercial additive manufacturing processes^[191]. The 3D models (inlets, outlets, and a box-like container) for stereolithography were designed in Blender CAD software^[192]. Han *et al.* developed a vascular network by adhering to a set of comprehensive design rules to design a blood vessel network on a skin patch^[193].

Some of the advantages of vat polymerization are the improved the manufacturing rate and the ability to generate objects with smooth surface (overall high resolution), which overcome major disadvantages of contemporary additive manufacturing. The limitation of this method is the diameter of the vessel that needs to be narrowed down to a range of 100 – 400 μm ^[192]. It is important to note that comprehensive studies on using vat polymerization to rebuild blood vessel are scarce. Besides, the materials with low stiffness are suitable to rebuild the soft tissue that needs better cell viability, while stronger materials are used in stereolithography to achieve high-resolution construction, which hinders the application of this method in blood vessel bioprinting.

4.4. Freeform reversible embedding of suspended hydrogel (FRESH)

To bioprint the complex blood vessel structures, FRESH is a method using a thermoreversible support bath to enable deposition of hydrogels^[194]. The technique revolves around printing a structure in the support bath to maintain the expected structure and printing fidelity^[195]. The thermoreversible support bath is made of gelatin particles, which is similar to Bingham plastics, and they behave as rigid bodies at low shear stresses but as viscous fluids at higher shear stresses^[196]. These properties ensure that the bath is at a low mechanical resistance when the needle moves across, while the hydrogel is kept in place after being extruded from the nozzle at 22°C. After completing the structure, the temperature is increased to 37°C and the gelatin will melt in a nondestructive manner. This method requires that the bioink must gel quickly to a fine wire without spreading in the support bath. Hinton *et al.* used the alginate- CaCl_2 (0.16%) system to print in the FRESH and obtained the $199 \pm 41 \mu\text{m}$ fine wire, and fabricated the right coronary artery vascular tree with a wall thickness of <1 mm, as shown in Figure 11^[196]. Lee *et al.* also used the FRESH to design the human heart components of all sizes, from the capillaries to the whole organs^[197]. Following the regulation of the collagen pH, the resolution of fabricated items could reach up to 10 microns with cells, and the microvessels fabricated using FRESH had optimal mechanical strength and cell viability^[197].

5. Conclusion and future perspectives

Bioprinting has an important place in the field of tissue repair due to its ability to spatially deposit biological materials in a layer-by-layer manner. Bioinks are a core aspect of bioprinting because they undertake the responsibilities in organizational formation and supporting cell viability. Therefore, bioink consists of special elements, such as ECM component and nutrient substance. The ideal bioink should have better printability, high degree of biocompatibility and biodegradability, as well as can be completely cured by cell-friendly treatment. Designing the ideal bioinks that have high mechanical strength and can support cell migration or proliferation is highly challenging. Until now, various kinds of hydrogel have been introduced in this area, such as the HA, collagen, alginate, fibrous protein, and dECM. However, it is hard for these materials to simulate the natural ECM due to the complex topologies and components. The dECM is a promising bioink material with bionic properties for establishing artificial blood vessel; however, enhancing support capability is a challenge. Common methods for addressing this include increasing the concentration of the dECM, adding biological molecules such as HA, collagen or alginate, or changing the cross-linking method.

The ultimate objective of 3D bioprinting is to print the injured or damaged organ *in situ*. At recent stage, only bioprinting of the shallow tissue (such as skin, cornea, or cartilage) is almost achievable. In regard to the artificial blood vessel, the current technology is only capable of pre-fabrication and further *in vitro* maturation before implantation. In the *in situ* printing of blood vessel, a faster cross-linking method is needed in the FSCR system, which needs to be combined with the scanning system and 3D rebuild software. Besides, more attention should be paid to the sterilization and safety of the *in situ* bioprinting systems.

The challenges that hinder the development of artificial blood vessel are the regulatory processes and funding approval. The Current Good Tissue Practice for human cell, tissue, and cellular and tissue-based product by the FDA requires that the bioinks must be manufactured in adherence to the stipulated guideline. For example, the preparation of bioink and cells should be more than 1 – 3 months, and *in vitro* cell culture may lead to unexpected cell differentiation, increase the risk of infection, and raise the production cost. Besides, the FDA guidelines clearly require that no more than 1 living microbe can be detected in every million sterilized final products of the blood vessel prosthesis. Therefore, for bioinks made by natural materials, sterilization technique is the final difficult aspect

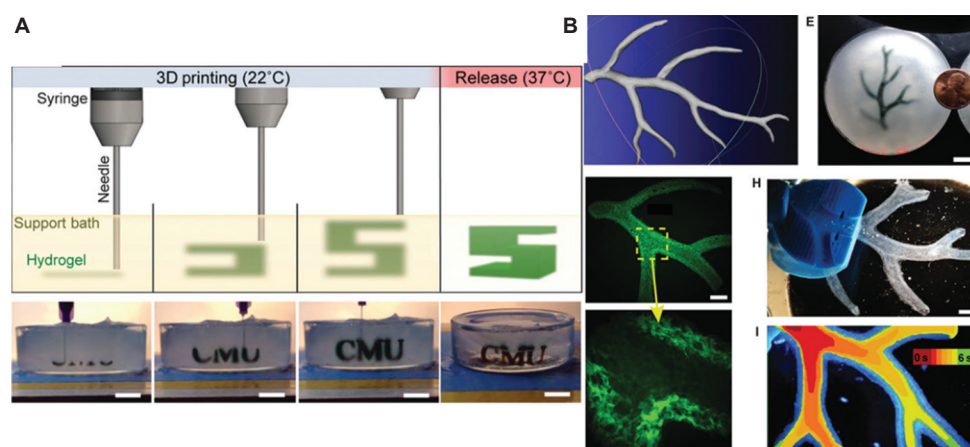


Figure 11. (A) A schematic of the freeform reversible embedding of suspended hydrogels (FRESH) process showing the hydrogel (green) being extruded and cross-linked within the gelatin slurry support bath (yellow). (B) A model of a section of a human right coronary arterial tree from 3D magnetic resonance imaging is processed at full scale into machine code for FRESH printing^[196].

that needs to be addressed. Some researchers found that the autoclave sterilization is the most destructive method, which will significantly reduce the viscosity and mechanical properties after cross-linking. Only ethylene oxide is the least destructive sterilization method, especially for the photo-cross-linking materials, such as HAMA and GelMA. Ethylene oxide could wipe out *Escherichia coli* without causing a decrease in viability and proliferation of MSCs. More importantly, the lack of manufacturing standards for bioprinting process is a great challenge to 3D bioprinting on a clinically relevant scale. Meanwhile, it is difficult to obtain regulatory approval for bioprinted blood vessels, given the complex clinical operation environment.

In the future, the construction of artificial blood vessels should fully consider the beneficial properties of natural materials, with a focus on adjustable mechanical properties and biocompatibility. As the barriers are being gradually overcome, using minimum number of components and simple designs in clinical applications will become possible.

Acknowledgment

None.

Funding

This work was supported by the National Natural Science Foundation of China (No. 82222007, 82170281 and U2004203), the Henan Thousand Talents Program (No. ZYQR201912131), Excellent Youth Science Foundation of Henan Province (No. 202300410362), Central Plains Youth Top Talent, Advanced funds (No.2021-CCA-ACCESS-125), Henan Province Medical Science and Technology Key Joint Project (SBGJ202101012), and the Key Scientific and Technological Research Projects in Henan Province (222102230025).

Conflict of interest

There are no conflicts of interest.

Author contributions

Conceptualization: Ya-Chen Hou and Jing-An Li

Funding acquisition: Jin-Ying Zhang, Jun-Nan Tang, and Jing-An Li

Investigation: Ya-Chen Hou, Jing-An Li, Xiaolin Cui, Zhen Qin, Chang Su, and Ge Zhang

Project administration: Jing-An Li, Jun-Nan Tang, and Jin-Ying Zhang

Supervision: Jing-An Li, Jun-Nan Tang, and Jin-Ying Zhang

Visualization: Ya-Chen Hou and Jing-An Li

Writing – original draft: Ya-Chen Hou

Writing – review and editing: Jing-An Li and Jun-Nan Tang

Ethics approval and consent to participate

Not applicable.

Consent for publication

Not applicable.

Availability of data

Not applicable.

References

- Jagannathan R, Patel SA, Ali MK, *et al.*, 2019, Global updates on cardiovascular disease mortality trends and attribution of traditional risk factors. *Curr Diab Rep*, 19: 44.
<https://doi.org/10.1007/s11892-019-1161-2>
- Matthews S, BATTERY A, O'Neil A, *et al.*, 2022, Sex differences in mortality after first time, isolated coronary artery bypass graft

- surgery: A systematic review and meta-analysis of randomized controlled trials. *Eur J Cardiovasc Nurs*, Online ahead of print: zvac028.
<https://doi.org/10.1093/eurjcn/zvac028>
3. Laschke MW, Menger MD, 2012, Vascularization in tissue engineering: Angiogenesis versus inosculation. *Eur Surg Res*, 48: 85–92.
<https://doi.org/10.1159/000336876>
 4. Lopes SV, Collins MN, Reis RL, *et al.*, 2021, Vascularization approaches in tissue engineering: Recent developments on evaluation tests and modulation. *ACS Appl Bio Mater*, 4: 2941–2956.
<https://doi.org/10.1021/acsabm.1c00051>
 5. Datta SK, Tumilowicz JJ, Trentin JJ, 1993, Lysis of human arterial smooth muscle cells infected with herpesviridae by peripheral blood mononuclear cells: Implications for atherosclerosis. *Viral Immunol*, 6: 153–160.
<https://doi.org/10.1089/vim.1993.6.153>
 6. Wang D, Xu Y, Li Q, *et al.*, 2020, Artificial small-diameter blood vessels: Materials, fabrication, surface modification, mechanical properties, and bioactive functionalities. *J Mater Chem B*, 8: 1801–1822.
<https://doi.org/10.1039/c9tb01849b>
 7. Kaplan J, Wagner R, White LE, *et al.*, 2021, Recurrent brachial artery aneurysm repair in a child managed with Gore-Tex conduit reinforcement. *J Vasc Surg Cases Innov Tech*, 7: 295–297.
<https://doi.org/10.1016/j.jvscit.2020.12.023>
 8. Ferrari G, Balasubramanian P, Tubaldi E, *et al.*, 2019, Experiments on dynamic behaviour of a Dacron aortic graft in a mock circulatory loop. *J Biomech*, 86: 132–140.
<https://doi.org/10.1016/j.jbiomech.2019.01.053>
 9. Careddu L, Petridis FD, Angeli E, *et al.*, 2019, Dacron conduit for extracardiac total cavopulmonary anastomosis: A word of caution. *Heart Lung Circ*, 28:1872–1880.
<https://doi.org/10.1016/j.hlc.2018.11.005>
 10. Zhang F, Xie Y, Celik H, *et al.*, 2019, Engineering small-caliber vascular grafts from collagen filaments and nanofibers with comparable mechanical properties to native vessels. *Biofabrication*, 11: 035020.
<https://doi.org/10.1088/1758-5090/ab15ce>
 11. Biazar E, Najafi SM, Heidari KS, *et al.*, 2018, 3D bio-printing technology for body tissues and organs regeneration. *J Med Eng Technol*, 42: 187–202.
<https://doi.org/10.1080/03091902.2018.1457094>
 12. Fukunishi T, Best CA, Sugiura T, *et al.*, 2017, Preclinical study of patient-specific cell-free nanofiber tissue-engineered vascular grafts using 3-dimensional printing in a sheep model. *J Thorac Cardiovasc Surg*, 153: 924–932.
<https://doi.org/10.1016/j.jtcvs.2016.10.066>
 13. Habib MA, Khoda B, 2022, Rheological analysis of bio-ink for 3D bio-printing processes. *J Manuf Process*, 76: 708–718.
<https://doi.org/10.1016/j.jmapro.2022.02.048>
 14. Schwab A, Levato R, D'Este M, *et al.*, 2020, Printability and shape fidelity of bioinks in 3D bioprinting. *Chem Rev*, 120: 11028–11055.
<https://doi.org/10.1021/acs.chemrev.0c00084>
 15. GhavamiNejad A, Ashammakhi N, Wu XY, *et al.*, 2020, Crosslinking strategies for 3D bioprinting of polymeric hydrogels. *Small*, 16: e2002931.
<https://doi.org/10.1002/smll.202002931>
 16. Olayanju A, Miller AF, Ansari T, *et al.*, 2021, Self-assembling Peptide Hydrogels-Peptigels® as a Platform for Hepatic Organoid Culture. *bioRxiv*, preprint.
<https://doi.org/10.1101/2021.03.01.433333>
 17. Wang Y, Li J, Li Y, *et al.*, 2021, Biomimetic bioinks of nanofibrillar polymeric hydrogels for 3D bioprinting. *Nano Today*, 39: 101180.
<https://doi.org/10.1016/j.nantod.2021.101180>
 18. Jia J, Richards DJ, Pollard S, *et al.*, 2014, Engineering alginate as bioink for bioprinting. *Acta Biomater*, 10: 4323–4331.
<https://doi.org/10.1016/j.actbio.2014.06.034>
 19. Jang J, Kim TG, Kim BS, *et al.*, 2016, Tailoring mechanical properties of decellularized extracellular matrix bioink by Vitamin B2-induced photo-crosslinking. *Acta Biomater*, 33: 88–95.
<https://doi.org/10.1016/j.actbio.2016.01.013>
 20. Lee H, Han W, Kim H, *et al.*, 2017, Development of liver decellularized extracellular matrix bioink for three-dimensional cell printing-based liver tissue engineering. *Biomacromolecules*, 18: 1229–1237.
<https://doi.org/10.1021/acs.biomac.6b01908>
 21. Lee J, Oh SJ, An SH, *et al.*, 2020, Machine learning-based design strategy for 3D printable bioink: Elastic modulus and yield stress determine printability. *Biofabrication*, 12: 035018.
<https://doi.org/10.1088/1758-5090/ab8707>
 22. Kuang H, Wang Y, Shi Y, *et al.*, 2020, Construction and performance evaluation of Hep/silk-PLCL composite nanofiber small-caliber artificial blood vessel graft. *Biomaterials*, 259: 120288.
<https://doi.org/10.1016/j.biomaterials.2020.120288>
 23. Wei LN, Chee KC, Shen YF, *et al.*, 2019, Print me an organ! Why we are not there yet. *Pro Polym Sci*, 97: 101145.
<https://doi.org/10.1016/j.progpolymsci.2019.101145>

24. Syedain ZH, Prunty A, Li J, *et al.*, 2021, Evaluation of the probe burst test as a measure of strength for a biologically-engineered vascular graft. *J Mech Behav Biomed Mater*, 119: 104527.
<https://doi.org/10.1016/j.jmbbm.2021.104527>
25. Konig G, McAllister TN, Dusserre N, *et al.*, 2009, Mechanical properties of completely autologous human tissue engineered blood vessels compared to human saphenous vein and mammary artery. *Biomaterials*, 30: 1542–1550.
<https://doi.org/10.1016/j.biomaterials.2008.11.011>
26. Matthew JM, Richard PT, Yang NJ, *et al.*, 2022, Bioengineering artificial blood vessels from natural materials. *Trends Biotechnol*, 40: 693–707.
<https://doi.org/10.1016/j.tibtech.2021.11.003>
27. Zandi N, Sani ES, Mostafavi E, *et al.*, 2021, Nanoengineered shear-thinning and bioprintable hydrogel as a versatile platform for biomedical applications. *Biomaterials*, 267: 120476.
<https://doi.org/10.1016/j.biomaterials.2020.120476>
28. Yoneyama T, Ito M, Sugihara K, *et al.*, 2000, Small diameter vascular prosthesis with a nonthrombogenic phospholipid polymer surface: Preliminary study of a new concept for functioning in the absence of pseudo-or neointima formation. *Artif Organs*, 24: 23–28.
<https://doi.org/10.1046/j.1525-1594.2000.06433.x>
29. Garcia-Cruz MR, Postma A, Frith JE, *et al.*, 2021, Printability and bio-functionality of a shear thinning methacrylated xanthan-gelatin composite bioink. *Biofabrication*, 13: 035023.
<https://doi.org/10.1088/1758-5090/abec2d>
30. Amorim PA, D'Ávila MA, Anand R, *et al.*, 2021, Insights on shear rheology of inks for extrusion-based 3D bioprinting. *Bioprinting*, 22: e00129.
<https://doi.org/10.1016/j.bprint.2021.e00129>
31. Bae M, Hwang DW, Ko MK, *et al.* 2021, Neural stem cell delivery using brain-derived tissue-specific bioink for recovering from traumatic brain injury. *Biofabrication*, 13: 044110.
<https://doi.org/10.1088/1758-5090/ac293f>
32. Diamantides N, Dugopolski C, Blahut E, *et al.*, 2019, High density cell seeding affects the rheology and printability of collagen bioinks. *Biofabrication*, 11: 045016.
<https://doi.org/10.1088/1758-5090/ab3524>
33. Xu C, Zhang M, Huang Y, *et al.*, 2014, Study of droplet formation process during drop-on-demand inkjetting of living cell-laden bioink. *Langmuir*, 30: 9130–9138.
<https://doi.org/10.1021/la501430x>
34. Gao T, Gillispie GJ, Copus JS, *et al.*, 2018, Optimization of gelatin-alginate composite bioink printability using rheological parameters: A systematic approach. *Biofabrication*, 10: 034106.
<https://doi.org/10.1088/1758-5090/aacdc7>
35. Zhang S, Li G, Man J, *et al.*, 2020, Fabrication of microspheres from high-viscosity bioink using a novel microfluidic-based 3D bioprinting nozzle. *Micromachines (Basel)*, 11: 681.
<https://doi.org/10.3390/mi11070681>
36. Skardal A, Zhang J, Prestwich GD, 2010, Bioprinting vessel-like constructs using hyaluronan hydrogels crosslinked with tetrahedral polyethylene glycol tetracrylates. *Biomaterials*, 31: 6173–6181.
<https://doi.org/10.1016/j.biomaterials.2010.04.045>
37. Liu W, Heinrich MA, Zhou Y, *et al.*, 2017, Extrusion bioprinting of shear-thinning gelatin methacryloyl bioinks. *Adv Healthc Mater*, 6: 1601451.
<https://doi.org/10.1002/adhm.201601451>
38. Lim W, Kim GJ, Kim HW, *et al.*, 2020, Kappa-carrageenan-based dual crosslinkable bioink for extrusion type bioprinting. *Polymers (Basel)*, 12: 2377.
<https://doi.org/10.3390/polym12102377>
39. Colosi C, Shin SR, Manoharan V, *et al.*, 2016, Microfluidic bioprinting of heterogeneous 3D tissue constructs using low-viscosity bioink. *Adv Mater*, 28: 677–684.
<https://doi.org/10.1002/adma.201503310>
40. Zhou K, Sun Y, Yang J, *et al.*, 2022, Hydrogels for 3D embedded bioprinting: A focused review on bioinks and support baths. *J Mater Chem B*, 10: 1897–1907.
<https://doi.org/10.1039/d1tb02554f>
41. Hoch E, Tovar GE, Borchers K, 2014, Bioprinting of artificial blood vessels: current approaches towards a demanding goal. *Eur J Cardiothorac Surg*, 46: 767–778.
<https://doi.org/10.1093/ejcts/ezu242>
42. Xing HA, Yz A, Ms A, *et al.*, 2021, A highly biocompatible bio-ink for 3D hydrogel scaffolds fabrication in the presence of living cells by two-photon polymerization. *Eur Polym J*, 153: 110505.
<https://doi.org/10.1016/j.eurpolymj.2021.110505>
43. Billiet T, Gevaert E, De Schryver T, *et al.*, 2014, The 3D printing of gelatin methacrylamide cell-laden tissue-engineered constructs with high cell viability. *Biomaterials*, 35: 49–62.
<https://doi.org/10.1016/j.biomaterials.2013.09.078>
44. Wang Z, Kumar H, Tian Z, *et al.*, 2018, Visible light photoinitiation of cell-adhesive gelatin methacryloyl hydrogels for stereolithography 3D bioprinting. *ACS Appl Mater Interfaces*, 10: 26859–26869.
<https://doi.org/10.1021/acsami.8b06607>

45. Deo KA, Singh KA, Peak CW, *et al.* 2020, Bioprinting 101: Design, fabrication, and evaluation of cell-laden 3D bioprinted scaffolds. *Tissue Eng Part A*, 26: 318–338.
<https://doi.org/10.1089/ten.TEA.2019.0298>
46. Wu J, Hu C, Tang Z, *et al.*, 2018, Tissue-engineered vascular grafts: Balance of the four major requirements. *Colloid Interface Sci Commun*, 23: 34–44.
<https://doi.org/10.1016/j.colcom.2018.01.005>
47. Sarkar S, Salacinski HJ, Hamilton G, *et al.*, 2006, The mechanical properties of infrainguinal vascular bypass grafts: Their role in influencing patency. *Eur J Vasc Endovasc Surg*, 31: 627–636.
<https://doi.org/10.1016/j.ejvs.2006.01.006>
48. Zhang Y, Yu Y, Ozbolat IT, 2013, Direct bioprinting of vessel-like tubular microfluidic channels. *J Nanotechnol Eng Med*, 4: 020902.
<https://doi.org/10.1115/1.4024398>
49. Liu Y, Li Z, Li J, *et al.*, 2020, Stiffness-mediated mesenchymal stem cell fate decision in 3D-bioprinted hydrogels. *Burns Trauma*, 8: tkaa029.
<https://doi.org/10.1093/burnst/tkaa029>
50. Lin CH, Su JJ, Lee SY, *et al.* 2018, Stiffness modification of photopolymerizable gelatin-methacrylate hydrogels influences endothelial differentiation of human mesenchymal stem cells. *J Tissue Eng Regen Med*, 12: 2099–2111.
<https://doi.org/10.1002/term.2745>
51. Ogle ME, Doron G, Levy MJ, *et al.*, 2020, Hydrogel culture surface stiffness modulates mesenchymal stromal cell secretome and alters senescence. *Tissue Eng Part A*, 26: 1259–1271.
<https://doi.org/10.1089/ten.tea.2020.0030>
52. Engler AJ, Sen S, Sweeney HL, *et al.*, 2006, Matrix elasticity directs stem cell lineage specification. *Cell*, 126: 677–689.
<https://doi.org/10.1016/j.cell.2006.06.044>
53. Yi B, Shen Y, Tang H, *et al.*, 2020, Stiffness of the aligned fibers affects structural and functional integrity of the oriented endothelial cells. *Acta Biomater*, 108: 237–249.
<https://doi.org/10.1016/j.actbio.2020.03.022>
54. Liu P, Tu J, Wang W, *et al.*, 2022, Effects of mechanical stress stimulation on function and expression mechanism of osteoblasts. *Front Bioeng Biotechnol*, 10: 830722.
<https://doi.org/10.3389/fbioe.2022.830722>
55. Matthews BD, Overby DR, Mannix R, *et al.*, 2006, Cellular adaptation to mechanical stress: Role of integrins, Rho, cytoskeletal tension and mechanosensitive ion channels. *J Cell Sci*, 119: 508–518.
<https://doi.org/10.1242/jcs.02760>
56. Yang Y, Beqaj S, Kemp P, *et al.*, 2000, Stretch-induced alternative splicing of serum response factor promotes bronchial myogenesis and is defective in lung hypoplasia. *J Clin Invest*, 106: 1321–1330.
<https://doi.org/10.1172/jci8893>
57. Sonam S, Sathe SR, Yim EK, *et al.*, 2016, Cell contractility arising from topography and shear flow determines human mesenchymal stem cell fate. *Sci Rep*, 6: 20415.
<https://doi.org/10.1038/srep20415>
58. Liang Y, Zhen X, Wang K, *et al.*, 2017, Folic acid attenuates cobalt chloride-induced pge2 production in huvecs via the no/hif-1alpha/cox-2 pathway. *Biochem Biophys Res Commun*, 490: 567–573.
<https://doi.org/10.1016/j.bbrc.2017.06.079>
59. Ogura Y, Sutterwala FS, Flavell RA, 2006, The inflammasome: First line of the immune response to cell stress. *Cell*, 126: 659–662.
<https://doi.org/10.1016/j.cell.2006.08.002>
60. Guilak F, Cohen DM, Estes BT, *et al.*, 2009, Control of stem cell fate by physical interactions with the extracellular matrix. *Cell Stem Cell*, 5: 17–26.
<https://doi.org/10.1016/j.stem.2009.06.016>
61. Young AT, White OC, Daniele MA, 2020, Rheological properties of coordinated physical gelation and chemical crosslinking in gelatin methacryloyl (GelMA) hydrogels. *Macromol Biosci*, 20: e2000183.
<https://doi.org/10.1002/mabi.202000183>
62. Marga F, Jakab K, Khatiwala C, *et al.*, 2012, Toward engineering functional organ modules by additive manufacturing. *Biofabrication*, 4: 022001.
<https://doi.org/10.1088/1758-5082/4/2/022001>
63. Gentile C, Lim KS, Vozzi G, 2021, Editorial: 3D bioprinting of vascularized tissues for *in vitro* and *in vivo* applications. *Front Bioeng Biotechnol*, 9: 754124.
<https://doi.org/10.3389/fbioe.2021.754124>
64. Shinohara S, Kihara T, Sakai S, *et al.*, 2013, Fabrication of *in vitro* three-dimensional multilayered blood vessel model using human endothelial and smooth muscle cells and high-strength PEG hydrogel. *J Biosci Bioeng*, 116: 231–234.
<https://doi.org/10.1016/j.jbiosc.2013.02.013>
65. Moore KH, Murphy HA, George EM, 2021, The glycocalyx: A central regulator of vascular function. *Am J Physiol Regul Integr Comp Physiol*, 320: R508–R518.
<https://doi.org/10.1152/ajpregu.00340.2020>
66. Xu Y, Hu Y, Liu C, *et al.*, 2018, A novel strategy for creating tissue-engineered biomimetic blood vessels using 3D bioprinting technology. *Materials (Basel)*, 11: 1581.

- <https://doi.org/10.3390/ma11091581>
67. Stanton M, Samitier J, Sanchez SJ, 2015, Bioprinting of 3D hydrogels. *Lab Chip*, 15: 3111–3115.
<https://doi.org/10.1039/C5LC90069G>
68. Rees A, Powell LC, Chinga-Carrasco G, *et al.*, 2015, 3D Bioprinting of carboxymethylated-periodate oxidized nanocellulose constructs for wound dressing applications. *Biomed Res Int*, 2015: 925757.
<https://doi.org/10.1155/2015/925757>
69. Sakai T, Matsunaga T, Yamamoto Y, *et al.*, 2008, Design and fabrication of a high-strength hydrogel with ideally homogeneous network structure from tetrahedron-like macromonomers. *Macromolecules*, 41: 5379–5384.
<https://doi.org/10.1021/ma800476x>
70. Kačarević ŽP, Rider PM, Alkildani S, *et al.*, 2018, An introduction to 3D bioprinting: Possibilities, challenges and future aspects. *Materials (Basel)*, 11: 2199.
<https://doi.org/10.3390/ma11112199>
71. Kim P, Yuan A, Nam KH, *et al.*, 2014, Fabrication of poly(ethylene glycol): gelatin methacrylate composite nanostructures with tunable stiffness and degradation for vascular tissue engineering. *Biofabrication*, 6: 024112.
<https://doi.org/10.1088/1758-5082/6/2/024112>
72. Li X, Liu X, Josey B, *et al.*, 2014, Short laminin peptide for improved neural stem cell growth. *Stem Cell Transl Med*, 3: 662–670.
<https://doi.org/10.5966/sctm.2013-0015>
73. Yamaoka T, Tabata Y, Ikada Y, 1994, Distribution and tissue uptake of poly(ethylene glycol) with different molecular weights after intravenous administration to mice. *J Pharm Sci*, 83: 601–606.
<https://doi.org/10.1002/jps.2600830432>
74. Peak CW, Singh KA, Adlouni M, *et al.*, 2019, Printing therapeutic proteins in 3D using nanoengineered bioink to control and direct cell migration. *Adv Healthc Mater*, 8: e1801553.
<https://doi.org/10.1002/adhm.201801553>
75. Choi YJ, Park H, Ha DH, *et al.*, 2021, 3D bioprinting of *in vitro* models using hydrogel-based bioinks. *Polymers (Basel)*, 13: 366.
<https://doi.org/10.3390/polym13030366>
76. Thanh TN, Laowattanatham N, Ratanavaraporn J, *et al.*, 2022, Hyaluronic acid crosslinked with alginate hydrogel: A versatile and biocompatible bioink platform for tissue engineering. *Eur Polym J*, 166: 111027.
<https://doi.org/10.1016/j.eurpolymj.2022.111027>
77. Lafuente-Merchan M, Ruiz-Alonso S, Espona-Noguera A, *et al.*, 2021, Development, characterization and sterilisation of nanocellulose-alginate-(hyaluronic acid)-bioinks and 3D bioprinted scaffolds for tissue engineering. *Mater Sci Eng C Mater Biol Appl*, 126: 112160.
<https://doi.org/10.1016/j.msec.2021.112160>
78. Zhang T, Zhao W, Xiahou Z, *et al.*, 2021, Bioink design for extrusion-based bioprinting. *Appl Mater Today*, 25: 101227.
<https://doi.org/10.1016/j.apmt.2021.101227>
79. Petta D, D'Amora U, Ambrosio L, *et al.* 2020, Hyaluronic acid as a bioink for extrusion-based 3D printing. *Biofabrication*, 12: 032001.
<https://doi.org/10.1088/1758-5090/ab8752>
80. Oliveira H, Médina C, Stachowicz ML, *et al.*, 2021, Extracellular matrix (ECM)-derived bioinks designed to foster vasculogenesis and neurite outgrowth: Characterization and bioprinting. *Bioprinting*, 22: e00134.
<https://doi.org/10.1016/j.bprint.2021.e00134>
81. Noh I, Kim N, Tran HN, *et al.*, 2019, 3D printable hyaluronic acid-based hydrogel for its potential application as a bioink in tissue engineering. *Biomater Res*, 23: 3.
<https://doi.org/10.1186/s40824-018-0152-8>
82. Xu L, Varkey M, Jorgensen A, *et al.*, 2020, Bioprinting small diameter blood vessel constructs with an endothelial and smooth muscle cell bilayer in a single step. *Biofabrication*, 12: 045012.
<https://doi.org/10.1088/1758-5090/aba2b6>
83. Zhu W, Qu X, Zhu J, *et al.*, 2017, Direct 3D bioprinting of prevascularized tissue constructs with complex microarchitecture. *Biomaterials*, 124: 106–1015.
<https://doi.org/10.1016/j.biomaterials.2017.01.042>
84. Zhao L, Lee VK, Yoo SS, *et al.*, 2012, The integration of 3-D cell printing and mesoscopic fluorescence molecular tomography of vascular constructs within thick hydrogel scaffolds. *Biomaterials*, 33: 5325–5332.
<https://doi.org/10.1016/j.biomaterials.2012.04.004>
85. Thomas A, Orellano I, Lam T, *et al.*, 2020, Vascular bioprinting with enzymatically degradable bioinks via multi-material projection-based stereolithography. *Acta Biomater*, 117: 121–132.
<https://doi.org/10.1016/j.actbio.2020.09.033>
86. Lu D, Zeng Z, Geng Z, *et al.*, 2022, Macroporous methacrylated hyaluronic acid hydrogel with different pore sizes for *in vitro* and *in vivo* evaluation of vascularization. *Biomed Mater*, 17: 025006.
<https://doi.org/10.1088/1748-605X/ac494b>
87. Lee J, Lee SH, Kim BS, *et al.*, 2018, Development and evaluation of hyaluronic acid-based hybrid bio-ink for tissue regeneration. *Tissue Eng Regen Med*, 15: 761–769.

- <https://doi.org/10.1007/s13770-018-0144-8>
88. Kesti M, Müller M, Becher J, *et al.*, 2015, A versatile bioink for three-dimensional printing of cellular scaffolds based on thermally and photo-triggered tandem gelation. *Acta Biomater*, 11: 162–172.
<https://doi.org/10.1016/j.actbio.2014.09.033>
89. Poldervaart MT, Goversen B, De Ruijter M, *et al.*, 2017, 3D bioprinting of methacrylated hyaluronic acid (MeHA) hydrogel with intrinsic osteogenicity. *PLoS One*, 12: e0177628.
<https://doi.org/10.1371/journal.pone.0177628>
90. Ouyang L, Armstrong JPK, Lin Y, *et al.*, 2020, Expanding and optimizing 3D bioprinting capabilities using complementary network bioinks. *Sci Adv*, 6: 035045
<https://doi.org/10.1126/sciadv.abc5529>
91. Petta D, Armiento AR, Grijpma D, *et al.*, 2018, 3D bioprinting of a hyaluronan bioink through enzymatic-and visible light-crosslinking. *Biofabrication*, 10: 044104.
<https://doi.org/10.1088/1758-5090/aadf58>
92. Thakur A, Jaiswal MK, Peak, CW, *et al.*, 2016, Injectible shear-thinning nanoengineered hydrogels for stem cell delivery. *Nanoscale*, 8: 12362–12372.
<https://doi.org/10.1039/C6NR02299E>
93. Li C, Han X, Ma Z, *et al.*, 2022, Engineered customizable microvessels for progressive vascularization in large regenerative implants. *Adv Healthc Mater*, 11: e2101836.
<https://doi.org/10.1002/adhm.202101836>
94. Zhu J, 2010, Bioactive modification of poly(ethylene glycol) hydrogels for tissue engineering. *Biomaterials*, 31: 4639–4656.
<https://doi.org/10.1016/j.biomaterials.2010.02.044>
95. Aisenbrey EA, Bryant S, 2016, Mechanical loading inhibits hypertrophy in chondrogenically differentiating hMSCs within a biomimetic hydrogel. *J Mater Chem B*, 4: 3562–3574.
<https://doi.org/10.1039/C6TB00006A>
96. Highley CB, Rodell CB, Burdick JA, 2015, Direct 3D printing of shear-thinning hydrogels into self-healing hydrogels. *Adv Mater*, 27: 5075–5079.
<https://doi.org/10.1002/adma.201501234>
97. Rodell CB, Kaminski AL, Burdick JA, 2013, Rational design of network properties in guest-host assembled and shear-thinning hyaluronic acid hydrogels. *Biomacromolecules*, 14: 4125–4134.
<https://doi.org/10.1021/bm401280z>
98. Jlab C, Yza B, Jeabd E, *et al.*, 2021, Bioactive nanoparticle reinforced alginate/gelatin bioink for the maintenance of stem cell stemness. *Mater Sci Eng C Mater Biol Appl*, 126: 112193.
<https://doi.org/10.1016/j.msec.2021.112193>
99. Rodell CB, MacArthur JW, Dorsey SM, *et al.*, 2015, Shear-thinning supramolecular hydrogels with secondary autonomous covalent crosslinking to modulate viscoelastic properties *in vivo*. *Adv Funct Mater*, 25: 636–644.
<https://doi.org/10.1002/adfm.201403550>
100. Loebel C, Rodell CB, Chen MH, *et al.*, 2017, Shear-thinning and self-healing hydrogels as injectable therapeutics and for 3D-printing. *Nat Protoc*, 12: 1521–1541.
<https://doi.org/10.1038/nprot.2017.053>
101. Maxson EL, Young MD, Noble C, *et al.*, 2019, *In vivo* remodeling of a 3D-Bioprinted tissue engineered heart valve scaffold. *Bioprinting*, 16: e00059.
<https://doi.org/10.1016/j.bprint.2019.e00059>
102. Alexander B, Daulton TL, Genin GM, *et al.*, 2012, The nanometre-scale physiology of bone: Steric modelling and scanning transmission electron microscopy of collagen-mineral structure. *J R Soc Interface*, 9: 1774–1786.
<https://doi.org/10.1098/rsif.2011.0880>
103. Włodarczyk-Biegun MK, Del Campo A, 2017, 3D bioprinting of structural proteins. *Biomaterials*, 134: 180–201.
<https://doi.org/10.1016/j.biomaterials.2017.04.019>
104. Gaudet ID, Shreiber DI, 2012, Characterization of methacrylated Type-I collagen as a dynamic, photoactive hydrogel. *Biointerphases*, 7: 25.
<https://doi.org/10.1007/s13758-012-0025-y>
105. Ryan AJ, Gleeson JP, Matsiko A, *et al.*, 2015, Effect of different hydroxyapatite incorporation methods on the structural and biological properties of porous collagen scaffolds for bone repair. *J Anat*, 227: 732–745.
<https://doi.org/10.1111/joa.12262>
106. Murphy CM, Matsiko A, Haugh MG, *et al.*, 2012, Mesenchymal stem cell fate is regulated by the composition and mechanical properties of collagen-glycosaminoglycan scaffolds. *J Mech Behav Biomed Mater*, 11: 53–62.
<https://doi.org/10.1016/j.jmbbm.2011.11.009>
107. Muthusamy S, Kannan S, Lee M, *et al.*, 2021, 3D bioprinting and microscale organization of vascularized tissue constructs using collagen-based bioink. *Biotechnol Bioeng*, 118: 3150–3163.
<https://doi.org/10.1002/bit.27838>
108. Hsu S, Jamieson AM, 1993, Viscoelastic behaviour at the thermal sol-gel transition of gelatin. *Polymer*, 34: 2602–2608.
[https://doi.org/10.1016/0032-3861\(93\)90596-3](https://doi.org/10.1016/0032-3861(93)90596-3)
109. Zhang J, Qiao C, Ma X, *et al.*, 2017, Effect of salts on the thermal stability of physically crosslinked gelatin hydrogels. *Polym Korea*, 41: 702–708.
<https://doi.org/10.7317/pk.2017.41.4.702>
110. Van Den Bulcke AI, Bogdanov B, De Rooze N, *et al.*, 2000,

- Structural and rheological properties of methacrylamide modified gelatin hydrogels. *Biomacromolecules*, 1: 31–38.
<https://doi.org/10.1021/bm990017d>
111. Loessner D, Meinert C, Kaemmerer E, *et al.*, 2016, Functionalization, preparation and use of cell-laden gelatin methacryloyl-based hydrogels as modular tissue culture platforms. *Nat Protoc*, 11: 727–746.
<https://doi.org/10.1038/nprot.2016.037>
112. Wang Z, Jin X, Dai R, *et al.*, 2016, An ultrafast hydrogel photocrosslinking method for direct laser bioprinting. *RSC Adv*, 6: 21099–21104.
<https://doi.org/10.1039/C5RA24910D>
113. Sk MM, Das P, Panwar A, *et al.*, 2021, Synthesis and characterization of site selective photo-crosslinkable glycidyl methacrylate functionalized gelatin-based 3D hydrogel scaffold for liver tissue engineering. *Mater Sci Eng C Mater Biol Appl*, 123: 111694.
<https://doi.org/10.1016/j.msec.2020.111694>
114. Fedorovich NE, Oudshoorn MH, van Geemen D, *et al.*, 2009, The effect of photopolymerization on stem cells embedded in hydrogels. *Biomaterials*, 30: 344–353.
<https://doi.org/10.1016/j.biomaterials.2008.09.037>
115. Hennink WE, van Nostrum CF, 2002, Novel crosslinking methods to design hydrogels. *Adv Drug Deliv Rev*, 54: 13–36.
[https://doi.org/10.1016/s0169-409x\(01\)00240-x](https://doi.org/10.1016/s0169-409x(01)00240-x)
116. Rouillard AD, Berglund CM, Lee JY, *et al.*, 2011, Methods for photocrosslinking alginate hydrogel scaffolds with high cell viability. *Tissue Eng Part C Methods*, 17: 173–179.
<https://doi.org/10.1089/ten.TEC.2009.0582>
117. Camci-Unal G, Cuttica D, Annabi N, *et al.*, 2013, Synthesis and characterization of hybrid hyaluronic acid-gelatin hydrogels. *Biomacromolecules*, 14: 1085–1092.
<https://doi.org/10.1021/bm3019856>
118. Duan B, Kapetanovic E, Hockaday LA, *et al.*, 2014, Three-dimensional printed trileaflet valve conduits using biological hydrogels and human valve interstitial cells. *Acta Biomater*, 10: 1836–1846.
<https://doi.org/10.1016/j.actbio.2013.12.005>
119. Fan Y, Yue Z, Lucarelli E, *et al.*, 2020, Hybrid printing using cellulose nanocrystals reinforced GelMA/HAMA hydrogels for improved structural integration. *Adv Healthc Mater*, 9: e2001410.
<https://doi.org/10.1002/adhm.202001410>
120. Mouser VH, Levato R, Mensinga A, *et al.*, 2020, Bio-ink development for three-dimensional bioprinting of hetero-cellular cartilage constructs. *Connect Tissue Res*, 61: 137–151.
<https://doi.org/10.1080/03008207.2018.1553960>
121. Nguyen AK, Goering PL, Elespuru RK, *et al.*, 2020, The photoinitiator lithium phenyl (2,4,6-Trimethylbenzoyl) phosphinate with exposure to 405 nm light is cytotoxic to mammalian cells but not mutagenic in bacterial reverse mutation assays. *Polymer (Basel)*, 12: 1489.
<https://doi.org/10.3390/polym12071489>
122. Yin J, Yan M, Wang Y, *et al.*, 2018, 3D Bioprinting of low-concentration cell-laden gelatin methacrylate (GelMA) bioinks with a two-step cross-linking strategy. *ACS Appl Mater Interfaces*, 10: 6849–6857.
<https://doi.org/10.1021/acsami.7b16059>
123. Kirsch M, Birnstein L, Pepelanova I, *et al.*, 2019, Gelatin-methacryloyl (GelMA) formulated with human platelet lysate supports mesenchymal stem cell proliferation and differentiation and enhances the hydrogel's mechanical properties. *Bioengineering (Basel)*, 6: 76.
<https://doi.org/10.3390/bioengineering6030076>
124. Wüst S, Godla ME, Müller R, *et al.*, 2014, Tunable hydrogel composite with two-step processing in combination with innovative hardware upgrade for cell-based three-dimensional bioprinting. *Acta Biomater*, 10: 630–640.
<https://doi.org/10.1016/j.actbio.2013.10.016>
125. Jin Q, Jin G, Ju J, *et al.*, 2022, Bioprinting small-diameter vascular vessel with endothelium and smooth muscle by the approach of two-step crosslinking process. *Biotechnol Bioeng*, 119: 1673–1684.
<https://doi.org/10.1002/bit.28075>
126. Bupphathong S, Quiroz, C, Huang, W, *et al.*, 2022, Gelatin methacrylate hydrogel for tissue engineering applications-a review on material modifications. *Pharmaceuticals*, 15: 171.
<https://doi.org/10.3390/ph15020171>
127. Cui H, Zhu W, Huang Y, *et al.*, 2019, *In vitro* and *in vivo* evaluation of 3D bioprinted small-diameter vasculature with smooth muscle and endothelium. *Biofabrication*, 12: 015004.
<https://doi.org/10.1088/1758-5090/ab402c>
128. Ruther F, Distler T, Boccaccini AR, *et al.*, 2018, Biofabrication of vessel-like structures with alginate di-aldehyde-gelatin (ADA-GEL) bioink. *J Mater Sci Mater Med*, 30: 8.
<https://doi.org/10.1007/s10856-018-6205-7>
129. Zhuang P, Ng WL, An J, *et al.*, 2019, Layer-by-layer ultraviolet assisted extrusion-based (UAE) bioprinting of hydrogel constructs with high aspect ratio for soft tissue engineering applications. *PLoS One*, 12: e0216776.
<https://doi.org/10.1371/journal.pone.0216776>
130. Crapo PM, Gilbert TW, Badylak SF, 2011, An overview of tissue and whole organ decellularization processes. *Biomaterials*, 32: 3233–3243.

- <https://doi.org/10.1016/j.biomaterials.2011.01.057>
131. Choudhury D, Tun HW, Wang T, *et al.*, 2018, Organ-derived decellularized extracellular matrix: A game changer for bioink manufacturing? *Trends Biotechnol*, 36: 787–805.
<https://doi.org/10.1016/j.tibtech.2018.03.003>
132. Li C, Zheng Z, Jia J, *et al.*, 2022, Preparation and characterization of photocurable composite extracellular matrix-methacrylated hyaluronic acid bioink. *J Mater Chem B*, 10: 4242–4253.
<https://doi.org/10.1039/d2tb00548d>
133. Pati F, Jang J, Ha DH, *et al.*, 2014, Printing three-dimensional tissue analogues with decellularized extracellular matrix bioink. *Nat Commun*, 5: 3935.
<https://doi.org/10.1038/ncomms4935>
134. Wolf MT, Daly KA, Brennan-Pierce EP, *et al.*, 2012, A hydrogel derived from decellularized dermal extracellular matrix. *Biomaterials*, 33: 7028–7038.
<https://doi.org/10.1016/j.biomaterials.2012.06.051>
135. Bilozur ME, Hay ED, 1988, Neural crest migration in 3D extracellular matrix utilizes laminin, fibronectin, or collagen. *Dev Biol*, 125: 19–33.
[https://doi.org/10.1016/0012-1606\(88\)90055-3](https://doi.org/10.1016/0012-1606(88)90055-3)
136. Asakura A, Komaki M, Rudnicki M, 2001, Muscle satellite cells are multipotential stem cells that exhibit myogenic, osteogenic, and adipogenic differentiation. *Differentiation*, 68: 245–253.
<https://doi.org/10.1046/j.1432-0436.2001.680412.x>
137. Czyz J, Wobus A, 2001, Embryonic stem cell differentiation: the role of extracellular factors. *Differentiation*, 68: 167–174.
<https://doi.org/10.1046/j.1432-0436.2001.680404.x>
138. Swaminathan S, Hamid Q, Sun W, *et al.*, 2019, Bioprinting of 3D breast epithelial spheroids for human cancer models. *Biofabrication*, 11: 025003.
<https://doi.org/10.1088/1758-5090/aafc49>
139. Schmidt SK, Schmid R, Arkudas A, *et al.*, 2019, Tumor cells develop defined cellular phenotypes after 3D-bioprinting in different bioinks. *Cells*, 8: 1295.
<https://doi.org/10.3390/cels8101295>
140. Shin YJ, Shafraneck RT, Tsui JH, *et al.*, 2021, 3D bioprinting of mechanically tuned bioinks derived from cardiac decellularized extracellular matrix. *Acta Biomaterialia*, 119: 75–88.
<https://doi.org/10.1016/j.actbio.2020.11.006>
141. Hockaday LA, Kang KH, Colangelo NW, *et al.*, 2012, Rapid 3D printing of anatomically accurate and mechanically heterogeneous aortic valve hydrogel scaffolds. *Biofabrication*, 4: 035005.
<https://doi.org/10.1088/1758-5082/4/3/035005>
142. Budharaju H, Zennifer A, Sethuraman S, *et al.*, 2022, Designer DNA biomolecules as a defined biomaterial for 3D bioprinting applications. *Mater Horiz*, 9: 1141–1166.
<https://doi.org/10.1039/d1mh01632f>
143. Nagahara S, Matsuda TJ, 1996, Hydrogel formation via hybridization of oligonucleotides derivatized in water-soluble vinyl polymers. *Polym Gels Netw*, 4: 111–127.
[https://doi.org/10.1016/0966-7822\(96\)00001-9](https://doi.org/10.1016/0966-7822(96)00001-9)
144. Gelinsky M, 2018, Biopolymer Hydrogel Bioinks. Netherlands: Elsevier. p.125–136.
<https://doi.org/10.1016/B978-0-08-101103-4.00008-9>
145. Wu Y, Li C, Boldt F, *et al.*, 2014, Programmable protein-DNA hybrid hydrogels for the immobilization and release of functional proteins. *Chem Commun (Camb)*, 50: 14620–1462.
<https://doi.org/10.1039/c4cc07144a>
146. Li C, Faulkner-Jones A, Dun AR, *et al.*, 2015, Rapid formation of a supramolecular polypeptide-DNA hydrogel for *in situ* three-dimensional multilayer bioprinting. *Angew Chem Int Ed Engl*, 54: 3957–3961.
<https://doi.org/10.1002/anie.201411383>
147. Yang L, Dun AR, Martin KJ, *et al.*, 2012, Secretory vesicles are preferentially targeted to areas of low molecular SNARE density. *PLoS One*, 7: e49514.
<https://doi.org/10.1371/journal.pone.0049514>
148. Pérez-Ortín JE, Tordera V, Chávez S, 2019, Homeostasis in the Central Dogma of molecular biology: The importance of mRNA instability. *RNA Biol*, 16: 1659–1666.
<https://doi.org/10.1080/15476286.2019.1655352>
149. Park N, Kahn JS, Rice EJ, *et al.*, 2009, High-yield cell-free protein production from P-gel. *Nat Protoc*, 4: 1759–1770.
<https://doi.org/10.1038/nprot.2009.174>
150. De Melo BA, Jodat YA, Cruz EM, *et al.*, 2020, Strategies to use fibrinogen as bioink for 3D bioprinting fibrin-based soft and hard tissues. *Acta Biomater*, 117: 60–76.
<https://doi.org/10.1016/j.actbio.2020.09.024>
151. Zhao N, Suzuki A, Zhang X, *et al.*, 2019, Dual aptamer-functionalized *in situ* injectable fibrin hydrogel for promotion of angiogenesis via codelivery of vascular endothelial growth factor and platelet-derived growth factor-BB. *ACS Appl Mater Interfaces*, 11: 18123–18132.
<https://doi.org/10.1021/acsami.9b02462>
152. Murphy KC, Whitehead J, Zhou D, *et al.*, 2017, Engineering fibrin hydrogels to promote the wound healing potential of mesenchymal stem cell spheroids. *Acta Biomater*, 64: 176–186.
<https://doi.org/10.1016/j.actbio.2017.10.007>

153. Freeman S, Ramos R, Alexis Chando P, *et al.*, 2019, A bioink blend for rotary 3D bioprinting tissue engineered small-diameter vascular constructs. *Acta Biomater*, 95: 152–164.
<https://doi.org/10.1016/j.actbio.2019.06.052>
154. Li L, Qin S, Peng J, *et al.*, 2020, Engineering gelatin-based alginate/carbon nanotubes blend bioink for direct 3D printing of vessel constructs. *Int J Biol Macromol*, 145: 262–271.
<https://doi.org/10.1016/j.ijbiomac.2019.12.174>
155. Hickson TG, Polson A, 1968, Some physical characteristics of the agarose molecule. *Biochim Biophys Acta*, 165: 43–58.
[https://doi.org/10.1016/0304-4165\(68\)90186-4](https://doi.org/10.1016/0304-4165(68)90186-4)
156. Gadjanski I, Yodmuang S, Spiller K, *et al.*, 2013, Supplementation of exogenous adenosine 5'-triphosphate enhances mechanical properties of 3D cell-agarose constructs for cartilage tissue engineering. *Tissue Eng Part A*, 19: 2188–2200.
<https://doi.org/10.1089/ten.TEA.2012.0352>
157. López-Marcial GR, Zeng AY, Osuna C, *et al.*, 2018, Agarose-based hydrogels as suitable bioprinting materials for tissue engineering. *ACS Biomater Sci Eng*, 4: 3610–3616.
<https://doi.org/10.1021/acsbiomaterials.8b00903>
158. Forget A, Derme T, Mitterberger D, *et al.*, 2019, Architecture-inspired paradigm for 3D bioprinting of vessel-like structures using extrudable carboxylated agarose hydrogels. *Emerg Mater*, 2: 233–243.
<https://doi.org/10.1007/s42247-019-00045-5>
159. Sharma C, Bhardwaj NK, 2019, Bacterial nanocellulose: Present status, biomedical applications and future perspectives. *Mater Sci Eng C Mater Biol Appl*, 104: 109963.
<https://doi.org/10.1016/j.msec.2019.109963>
160. Klemm D, Kramer F, Moritz S, *et al.*, 2011, Nanocelluloses: A new family of nature-based materials. *Angew Chem Int Ed Engl*, 50: 5438–5466.
<https://doi.org/10.1002/anie.201001273>
161. Da Gama FM, Dourado F, 2018, Bacterial nanocellulose: What future? *Bioimpacts*, 8: 1–3.
<https://doi.org/10.15171/bi.2018.01>
162. Di Biase M, De Leonardi P, Castelletto V, *et al.*, 2011, Photopolymerization of pluronic F127 diacrylate: A colloid-templated polymerization. *Soft Matter*, 7: 4928–4937.
<https://doi.org/10.1039/C1SM05095H>
163. Malda J, Visser J, Melchels FP, *et al.*, 2013, 25th anniversary article: Engineering hydrogels for biofabrication. *Adv Mater*, 25: 5011–5028.
<https://doi.org/10.1002/adma.201302042>
164. Bohorquez M, Koch C, Trygstad T, *et al.*, 1999, A study of the temperature-dependent micellization of pluronic F127. *J Colloid Interface Sci*, 216:34–40. doi.org/10.1006/jcis.1999.6273
165. Liu Y, Zhang Y, Jiang W, *et al.*, 2019, A novel biodegradable multilayered bioengineered vascular construct with a curved structure and multi-branches. *Micromachines (Basel)*, 10: 275.
<https://doi.org/10.3390/mi10040275>
166. O'Connell CD, Konate S, Onofrillo C, *et al.*, 2020, Free-form co-axial bioprinting of a gelatin methacryloyl bioink by direct *in situ* photo-crosslinking during extrusion. *Bioprinting*, 19: e00087.
<https://doi.org/10.1016/j.bprint.2020.e00087>
167. Chen Y, Xiong X, Liu X, *et al.*, 2020, 3d bioprinting of shear-thinning hybrid bioinks with excellent bioactivity derived from gellan/alginate and thixotropic magnesium phosphate-based gels. *J Mater Chem B*, 8: 5500–5514.
<https://doi.org/10.1039/D0TB00060D>
168. Müller M, Becher J, Schnabelrauch M, *et al.*, 2015, Nanostructured pluronic hydrogels as bioinks for 3D bioprinting. *Biofabrication*, 7: 035006.
<https://doi.org/10.1088/1758-5090/7/3/035006>
169. Millik SC, Dostie AM, Karis DG, *et al.*, 2019, 3D printed coaxial nozzles for the extrusion of hydrogel tubes toward modeling vascular endothelium. *Biofabrication*, 11: 045009.
<https://doi.org/10.1088/1758-5090/ab2b4d>
170. Selmi TA, Verdonk P, Chambat P, *et al.*, 2008, Autologous chondrocyte implantation in a novel alginate-agarose hydrogel: Outcome at two years. *J Bone Joint Surg Br*, 90: 597–604.
<https://doi.org/10.1302/0301-620x.90b5.20360>
171. Remminghorst U, Rehm BH, 2006, Bacterial alginates: From biosynthesis to applications. *Biotechnol Lett*, 28: 1701–1712.
<https://doi.org/10.1007/s10529-006-9156-x>
172. Kang SM, Lee JH, Huh YS, *et al.*, 2021, Alginate microencapsulation for three-dimensional *in vitro* cell culture. *ACS Biomater Sci Eng*, 7: 2864–2879.
<https://doi.org/10.1021/acsbmaterials.0c00457>
173. Colosi C, Shin SR, Manoharan V, *et al.*, 2016, Microfluidic bioprinting of heterogeneous 3D tissue constructs using low-viscosity bioink. *Adv Mater*, 28: 677–684.
<https://doi.org/10.1002/adma.201503310>
174. Gao Q, Liu Z, Lin Z, *et al.*, 2017, 3D Bioprinting of vessel-like structures with multilevel fluidic channels. *ACS Biomater Sci Eng*, 3: 399–408.
<https://doi.org/10.1021/acsbmaterials.6b00643>
175. Jia W, Gungor-Ozkerim PS, Zhang YS, *et al.*, 2016, Direct 3D bioprinting of perfusable vascular constructs using a blend bioink. *Biomaterials*, 106: 58–68.

- <https://doi.org/10.1016/j.biomaterials.2016.07.038>
176. Zhang Y, Yu Y, Akkouch A, *et al.*, 2015, *In vitro* study of directly bioprinted perfusable vasculature conduits. *Biomater Sci*, 3: 134–143.
<https://doi.org/10.1039/c4bm00234b>
177. Jang EH, Kim JH, Lee JH, *et al.*, 2020, Enhanced biocompatibility of multi-layered, 3D bio-printed artificial vessels composed of autologous mesenchymal stem cells. *Polymers (Basel)*, 12: 538.
<https://doi.org/10.3390/polym12030538>
178. Karen D, Yuki H, Kazuomori KL, *et al.*, 2016, Dual-stage crosslinking of a gel-phase bioink improves cell viability and homogeneity for 3D bioprinting. *Adv Healthcare Mater*, 5: 2488–2492.
<https://doi.org/10.1002/adhm.201600636>
179. Tao J, Jose GM, Flores-Torres S, *et al.*, 2019, Extrusion bioprinting of soft materials: An emerging technique for biological model fabrication. *Appl Phys Rev*, 6: 011310.
<https://doi.org/10.1063/1.5059393>
180. Heinrich MA, Liu W, Jimenez A, *et al.*, 2019, 3D Bioprinting: From benches to translational applications. *Small*, 15: e1805510.
<https://doi.org/10.1002/smll.201805510>
181. Kalyani S, Kawal R, 2022, Could 3D extrusion bioprinting serve to be a real alternative to organ transplantation in the future? *Ann 3D Print Med*, 7: 100066.
<https://doi.org/10.1016/j.stlm.2022.100066>
182. Norotte C, Marga FS, Niklason LE, *et al.*, 2009, Scaffold-free vascular tissue engineering using bioprinting. *Biomaterials*, 30: 5910–5917.
<https://doi.org/10.1016/j.biomaterials.2009.06.034>
183. Park SJ, Lee J, Jae WC, *et al.*, 2021, Additive manufacturing of the core template for the fabrication of an artificial blood vessel: The relationship between the extruded deposition diameter and the filament/nozzle transition ratio. *Mater Sci Eng C*, 118: 111406.
<https://doi.org/10.1016/j.msec.2020.111406>
184. Trujillo S, Seow M, Lueckgen A, *et al.*, 2021, Dynamic mechanical control of alginate-fibronectin hydrogels with dual crosslinking: Covalent and ionic. *Polymers (Basel)*, 13: 433.
<https://doi.org/10.3390/polym13030433>
185. Li XD, Liu BX, Pei B, *et al.*, 2020, Inkjet bioprinting of biomaterials. *Chem Rev*, 120: 10793–10833.
<https://doi.org/10.1021/acs.chemrev.0c00008>
186. Bogala MR, 2022, Three-dimensional (3D) printing of hydroxyapatite-based scaffolds: A review. *Bioprinting*, 28: e00244.
<https://doi.org/10.1016/j.bprint.2022.e00244>
187. Arai K, Iwanaga S, Toda H, *et al.*, 2011, Three-dimensional inkjet biofabrication based on designed images. *Biofabrication*, 3: 034113.
<https://doi.org/10.1088/1758-5082/3/3/034113>
188. Ng WL, Huang X, Shkolnikov V, *et al.*, 2021, Controlling droplet impact velocity and droplet volume: Key factors to achieving high cell viability in sub-nanoliter droplet-based bioprinting. *Int J Bioprint*, 8: 424.
<https://doi.org/10.18063/ijb.v8i1.424>
189. Lee JM, Zhou MM, Chen YW, *et al.*, 2020, Vat polymerization-based bioprinting-process, materials, applications and regulatory challenges. *Biofabrication*, 12: 022001.
<https://doi.org/10.1088/1758-5090/ab6034>
190. Li W, Mille LS, Robledo JA, *et al.*, 2020, Recent advances in formulating and processing biomaterial inks for vat polymerization-based 3D printing. *Adv Healthc Mater*, 9: e2000156.
<https://doi.org/10.1002/adhm.202000156>
191. Joanna I, Marina V, Alessia P, *et al.*, 2021, Alginate-based tissue-specific bioinks for multi-material 3D-bioprinting of pancreatic islets and blood vessels: A step towards vascularized pancreas grafts. *Bioprinting*, 24: e00163.
<https://doi.org/10.1016/j.bprint.2021.e00163>
192. Costa PF, Hugo JA, John EAL, *et al.*, 2017, Mimicking arterial thrombosis in a 3D-printed microfluidic *in vitro* vascular model based on computed tomography angiography data. *Lab Chip*, 17: 2785–2792.
<https://doi.org/10.1039/C7LC00202E>
193. Han X, Courseaus J, Khamassi J, *et al.*, 2018, Optimized vascular network by stereolithography for tissue engineered skin. *Int J Bioprint*, 4: 134.
<https://doi.org/10.18063/IJB.v4i2.134>
194. Bhatia SK, Sharma S, 2014, 3D-printed prosthetics roll off the presses. *Chem Eng Prog*, 110: 28–33.
195. Wu W, DeConinck A, Lewis JA, 2011, Omnidirectional printing of 3D microvascular networks. *Adv Mater*, 23: H178–H183.
<https://doi.org/10.1002/adma.201004625>
196. Hinton TJ, Jallerat Q, Palchesko RN, *et al.*, 2015, Three-dimensional printing of complex biological structures by freeform reversible embedding of suspended hydrogels. *Sci Adv*, 1: e1500758.
<https://doi.org/10.1126/sciadv.1500758>
197. Lee A, Hudson AR, Shiwardski DJ, *et al.*, 2019, 3D bioprinting of collagen to rebuild components of the human heart. *Science*, 365: 482–487.
<https://doi.org/10.1126/science.aav9051>